HHS Public Access

Author manuscript

Exp Neurol. Author manuscript; available in PMC 2021 December 01.

Published in final edited form as:

Exp Neurol. 2020 December ; 334: 113437. doi:10.1016/j.expneurol.2020.113437.

The potassium channel Kv4.2 regulates dendritic spine morphology, electroencephalographic characteristics and seizure susceptibility in mice

Durgesh Tiwari[1,3], **Tori L. Schaefer**[2], **Lindsay M. Schroeder-Carter**[1], **Joseph C. Krzeski**[1], **Alexander T. Bunk**[1], **Emma V. Parkins**[1], **Andrew Snider**[1], **Reese Danzer**[1], **Michael T. Williams**[1,3], **Charles V. Vorhees**[1,3], **Steve C. Danzer**[3,4,5], **Christina Gross**[1,3]

[1]Division of Neurology, Cincinnati Children's Hospital Medical Center, Cincinnati, Ohio 45229, USA;

[2]Division of Psychiatry, Cincinnati Children's Hospital Medical Center, Cincinnati, Ohio 45229, USA;

[3]Department of Pediatrics, University of Cincinnati College of Medicine, Cincinnati, Ohio 45229, USA;

[4]Department of Anesthesia, Cincinnati Children's Hospital Medical Center, Cincinnati, Ohio 45229, USA;

[5]Department of Anesthesiology, University of Cincinnati College of Medicine, Cincinnati, Ohio 45267, USA

Abstract

The voltage-gated potassium channel Kv4.2 is a critical regulator of dendritic excitability in the hippocampus and is crucial for dendritic signal integration. Kv4.2 mRNA and protein expression as well as function are reduced in several genetic and pharmacologically induced rodent models of epilepsy and autism. It is not known, however, whether reduced Kv4.2 is just an epiphenomenon or a disease-contributing cause of neuronal hyperexcitability and behavioral impairments in these neurological disorders. To address this question, we used male and female mice heterozygous for a Kv.2 deletion and adult-onset manipulation of hippocampal Kv4.2 expression in male mice to assess the role of Kv4.2 in regulating neuronal network excitability, morphology and anxiety-related behaviors. We observed a reduction in dendritic spine density and reduced proportions of thin and stubby spines but no changes in anxiety, overall activity, or retention of conditioned freezing memory in Kv4.2 heterozygous mice compared with wildtype littermates. Using EEG analyses, we showed elevated theta power and increased spike frequency in Kv4.2 heterozygous mice under basal conditions. In addition, the latency to onset of kainic acid-induced seizures was

*Correspondence: Christina Gross: Cincinnati Children's Hospital Medical Center; Research Building, R.2407; 3333 Burnet Avenue, Cincinnati, OH 45229 Tel: (513) 636 3493 FAX: (513) 636 1888, christina.gross@cchmc.org.

Declarations of interest: none

significantly shortened in Kv4.2 heterozygous mice compared with wildtype littermates, which was accompanied by a significant increase in theta power. By contrast, overexpressing Kv4.2 in wildtype mice through intrahippocampal injection of Kv4.2-expressing lentivirus delayed seizure onset and reduced EEG power. These results suggest that Kv4.2 is an important regulator of neuronal network excitability and dendritic spine morphology, but not anxiety-related behaviors. In the future, manipulation of Kv4.2 expression could be used to alter seizure susceptibility in epilepsy.

Keywords

Kv4.2; A-type potassium channel; epilepsy; seizure; autism; dendritic spine morphology; lentiviral overexpression; electroencephalography

Introduction

Ion channels are critical modulators of excitability at cellular and circuit levels, and their investigation can provide essential insight into mechanisms underlying neurological disorders that involve hyperexcitability of the brain. *KCND2,* the gene encoding the voltage-gated potassium channel Kv4.2 has been suggested as a risk gene for epilepsy and autism in several gene profiling studies (Singh et al., 2006; Casey et al., 2012; Guo et al., 2012; Connolly et al., 2013; Lee et al., 2014). Kv4.2 mediates somatodendritic A-type potassium currents and plays a vital role in the regulation of neuronal excitability and dendritic signal integration in the hippocampus (Birnbaum et al., 2004; Chen et al., 2006). Besides gene mutations in *KCND2*, altered expression and function of Kv4.2 protein were also observed in mouse models for monogenic neurological disorders such as Fragile × Syndrome (Gross et al., 2011; Lee et al., 2011; Routh et al., 2013; Kalmbach et al., 2015) and PTEN deletion syndrome (Lugo et al., 2014). Both disorders are associated with autism and epilepsy, and their mouse models exhibit several autistic-like and anxiety-related behaviors. Moreover, reduced Kv4.2 expression was detected after acute seizures in mice and rats (Tsaur et al., 1992; Francis et al., 1997; Gross et al., 2016), and in animal models of acquired epilepsy such as traumatic brain injury (Lei et al., 2012) and pilocarpine-induced temporal lobe epilepsy (Bernard et al., 2004; Monaghan et al., 2008; Tiwari et al., 2019).

Hippocampal neurons from Kv4.2 knockout ($Kv4.2^{KO}$) mice show delayed synaptic maturation, have more silent (i.e. AMPA receptor-free) synapses, and their intrinsic excitability is increased (Chen et al., 2006; Kim and Hoffman, 2012). These synaptic deficits in the absence of Kv4.2 are also reflected behaviorally: $Kv4.2^{KO}$ mice have deficits in learning and memory suggesting a critical role of Kv4.2 in cognition (Lugo et al., 2012). The effect of Kv4.2 deletion on brain excitability is less clear: one study shows increased seizure susceptibility following kainic acid injection (Barnwell et al., 2009), but we did not detect differences in the latency to seizure onset using a similar paradigm (Gross et al., 2016). The ambiguous effect on seizure susceptibility may be due to compensatory changes on the brain circuit level in adult $Kv4.2^{KO}$ mice. Indeed, studies in $Kv4.2^{KO}$ mice have demonstrated that complete loss of Kv4.2 leads to downregulation of two of its auxiliary subunits, KChIP2 and 3 in the hippocampus (Menegola and Trimmer, 2006; Menegola et al.,

2012) and to increased hippocampal tonic GABA currents (Andrasfalvy et al., 2008). Changes on electrical and molecular levels were also observed in the heart of Kv4.2^{KO} mice (Guo et al., 2005). We hypothesized that Kv4.2 heterozygous mice (Kv4.2^{HET}) may be less prone to compensatory effects than Kv4.2^{KO} mice, in addition to better modeling the reduced levels (but not lack) of Kv4.2 observed in neurological disorders. Thus, they could be a more suitable model to assess Kv4.2-mediated effects on neuronal excitability in neurological disorders.

The aim of this study was to assess the role of reduced Kv4.2 in brain disorders such as autism and epilepsy by investigating the effect of Kv4.2 levels on neuronal morphology and network excitability, as well as on anxiety- and conditioned freezing related deficits. We show that reduced expression of Kv4.2 leads to reduced dendritic spine density and a more immature spine morphology, whereas anxiety-related behaviors and conditioned freezing memory are unchanged. Using EEG analyses, we demonstrate that reduced Kv4.2 levels increase basal and kainic acid-induced brain activity and increase susceptibility to seizures. By contrast, intrahippocampal CA1 injection of a lentivirus overexpressing Kv4.2 in wildtype mice delays seizure onset and reduces EEG theta power. Overall, our study reveals an important role of Kv4.2 in regulating network excitability and warrants future analyses into altered Kv4.2 as an underlying pathological mechanism in epilepsy.

Material and methods

Animals

All animal procedures were approved by the Institutional Animal Care and Use Committee of CCHMC and complied with the Guideline for the Care and Use of Laboratory Animals. Kv4.2^{KO} mice were obtained as a kind gift from Dr. Jeanne Nerbonne (Washington University, St Louis). Male heterozygous Kv4.2 (Kv4.2^{HET}) mice in C57BL/6J background and female C57BL/6J wildtype (WT) mice (Jackson stock number 000664, RRID: IMSR_JAX:000664) were bred at CCHMC to generate heterozygous Kv4.2 and WT littermates. Pups were weaned at P21–28 and were housed with same sex littermates (maximum 4 per cage) in a standard cage with food and water provided *ad libitum.* Mice were maintained on a 14:10 hour light:dark cycle, and all experiments were performed during the light cycle. Male Kv4.2^{HET} mice and WT littermates were used for all experiments, except for the analysis of nesting and marble burying behavior and the analysis of dendritic spine morphology where both male and female mice were used. For dendritic spine morphology analyses, female *thy1*-EGFP mice (B6.Cg-Tg(Thy1-EGFP)OJrs/GfngJ Jackson, catalogue no. 007919, RRID:IMSR_JAX:007919) and male Kv4.2^{HET} mice were used for breeding, and male and female *thy1*-EGFP-positive offspring was used at P60 for analysis. Male 6–8 week-old C57BL/6J WT mice were used for bilateral intrahippocampal CA1 injection of lentiviral particles.

Antibodies, drugs, lentiviral particles and primers

The following antibodies were used: mouse monoclonal anti-Kv4.2 (UC Davis/NIH NeuroMab Facility Cat# 75–016, RRID:AB_2131945), mouse monoclonal Kv4.3 (UC Davis/NIH NeuroMab Facility Cat# 75–017, RRID:AB_2131966), mouse monoclonal anti-

Akt (Cell Signaling Technology Cat# 2920, RRID:AB_1147620), mouse monoclonal anti-βActin (Sigma-Aldrich Cat# A1978, RRID:AB_476692), rabbit polyclonal anti-DPP6 (Abcam Cat# ab41809, RRID:AB_732017), rabbit polyclonal anti-DPP10 (Abcam Cat#ab42082, RRID:AB_2093405), mouse monoclonal anti-KChIP2 (UC Davis/NIH NeuroMab Facility Cat# 75–004, RRID:AB_10671304), and mouse monoclonal anti-KChIP3 (UC Davis/NIH NeuroMab Facility Cat# 75–005, RRID:AB_2130257). Secondary antibodies used for detection of western blot with chemiluminescence were obtained from GE Healthcare Life Sciences, Marlborough, MA, and for fluorescent detection from LI-COR, Lincoln, NB. Lentiviral particles expressing *Kcnd2* and control lentiviral particles (virus containing the empty vector) were obtained from GeneCopoeia (Cat# LPP-Mm03412-Lv105–100, and LPP-NEG-LV105–100-C). Kainic acid (cat# 0222) was obtained from Tocris Biosciences, MN, USA, and was dissolved in sterile Ringers (Hospira, IL, USA). Diazepam (cat# 1185008) was obtained from Sigma-Aldrich (St. Louis, MO). The following qRT-PCR primers were used: Kv4.2for: GCTTTGAGACACAGCACCAC; Kv4.2rev: TGTTCATCGACAAACTCATGG; β-tubfor: TCGTGGAATGGATCCCCAAC; β-tubrev: TCCATCTCGTCCATGCCCT.

RNA isolation and qRT-PCR

RNA was extracted from tissue punches using Trizol® (Life Technologies, Carlsbad, CA), and cDNA was generated using the High Capacity RNA-to-cDNA Kit (Applied Biosystems, Foster City, CA), followed by SYBR green quantitative real-time PCR (Bio-Rad Laboratories, Hercules, CA) using a QuantStudio 3 Real-Time PCR System (Applied Biosystems, Foster City, CA). Relative changes were quantified with the comparative cycle threshold method ($2^{-\Delta CT}$). Quality and quantity of mRNA was measured using a Nanodrop Spectrophotometer (Thermo Fisher Scientific, Waltham, MA). Reverse transcription for qPCRs was carried out using 1μg RNA.

Western blots

Western blots were done as described previously (Muddashetty et al., 2007) using lysates from the whole hippocampus of $Kv4.2^{HET}$ mice and their WT littermates. Kv4.2, Kv4.3, KChIP2, KChIP3, Akt and β-Actin were detected with HRP-coupled secondary antibodies and chemiluminescence. DDP6 and DPP10 were detected with fluorescent secondary antibodies. Specific bands were quantified using NIH ImageJ software and normalized to a loading control on the same gel. The loading control for Kv4.2, Kv4.3, DDP10 and KChIP2 was Akt, and for DPP6 and KChIP3 β-Actin or Akt. For DPP and KChIP detection, blots were cut in half after transfer. The top part was used for DPP detection, the bottom part for KChIP and β-Actin or Akt detection. All samples were run and quantified in duplicates.

Hippocampal tissue punches

To obtain CA1 hippocampal tissue punches from lentivirus-infected brains, whole brains were dissected, flash frozen and cut into slices of 1mm thickness with a coronal steel brain matrix (Stoelting Inc, Wood Dale, IL). Using a mouse brain stereotaxic atlas, the hippocampal CA1 region was identified (George Paxinos, 2012), dissected with a micro puncher (1 mm diameter, Harris-UniCore™, Electron Microscopy Sciences, Hartfield, PA),

and flash frozen on dry ice. Slices between bregma levels −1.5 to −2.5 mm were selected for the tissue dissection.

Dendritic spine density analysis

Male and female offspring from female *thy1*-EGFP positive and male Kv4.2^{HET} breeders were used at P60. Mice were transcardially perfused with 4% paraformaldehyde, and brains were dissected and postfixed overnight in 4% paraformaldehyde. 500 μm-thick coronal sections were prepared using a vibratome (VT1000S, Leica, Wetzlar, Germany), and sections were cleared using passive clearing technique (PACT) as described previously (Yang et al., 2014). Briefly, slices were incubated in 4% acrylamide hydrogel overnight, cleared with 8% SDS for 24 hours, washed and stored in 0.02% sodium azide at 4°C until mounting. Sections were mounted using Fluoromount-G® (SouthernBiotech, Birmingham, AL) and imaged on a Nikon A1R HD inverted microscope equipped with LUN-V laser launch using a 100x objective (Nikon Instruments, Inc, Melville, NY). Acquired z-stacks were deconvolved by blind 3D deconvolution (NIS-Elements, Nikon Instruments). Dendritic spines were analyzed on apical secondary dendrites of pyramidal neurons in the hippocampal CA1 area. Dendrites were analyzed for up to a total length of 100 μm or wherever the secondary dendrite ended. Overall spine density was quantified manually using Image J (NIH), and dendritic spine classification was performed semi-automatedly using Neurolucida®360 software (MBF Bioscience, Williston, VT) with a preset algorithm (Rodriguez et al., 2008; Dickstein et al., 2016). Five to six brains per genotype were analyzed with two to six neurons per brain (details in figure legends). Dendritic spine counts of all analyzed neurons from WT and Kv4.2^{HET} mice were pooled for statistical analysis. Dendritic spine analysis was performed by two independent experimenters with very comparable results.

Behavioral experiments

Anxiety- and autism-associated behavioral analyses were conducted in the following order on separate days: nesting, marble burying, elevated zero maze. A separate cohort was utilized to test for audiogenic seizures. A third cohort was used to test prepulse inhibition and fear conditioning. These experiments were performed using male Kv4.2^{HET} mice with WT littermate controls. In addition, a cohort of female Kv4.2^{HET} and WT littermates was used to assess nesting and marble burying. Experimenters and analyzers were blind to the genotype of the tested mice.

Nesting—Nesting behavior was assessed at 2 h and 24 h post nestlet placement as per described protocols (Deacon, 2006; Gross et al., 2015a). Before starting the test, mice were individually housed for a period of 3 days to acclimatize and avoid behavioral changes due to a novel environment. Nests were scored on a rating scale of 1 to 5 as described in Deacon, 2006. Briefly, a score of 1 indicates more than 90% intact nestlet, 2 indicates 50–90% nestlet remains intact, 3 indicates mostly shredded nestlets (>90%) with no identifiable nest, 4 indicates an identifiable nest with more than 90% nestlet torn and 5 represents a near perfect nest with walls taller than the mouse with more than 90% nestlet torn. In addition, the leftover nestlet was weighed and the percentage torn was calculated and compared. While

scoring is less objective than weighing used nestlet it captures the capability of a mouse to build a nest regardless of how much nestlet material was used.

Marble burying—Marble burying was assessed as described previously (Gross et al., 2015a). Briefly, rat cages (16in × 14in × 8in) were used for the test, and 20 dark blue glass marbles were arranged in a 4 × 5 grid pattern on 4 inches of standard cage bedding. Marbles covered 50% or more were recorded as buried. Latency to start burying and the number of marbles buried at 5, 10 and 15 min were recorded.

Elevated zero maze (EZM)—EZM was performed as per the protocol described in Schaefer et al 2009. The apparatus consisted of a circular runway with closed and open quadrants located on opposing ends. The runway was 5 cm wide with a 50 cm internal diameter and was elevated 40 cm above the floor with 0.5 cm curbs to prevent accidental slipping off the edge (San Diego Instruments, CA). The room light was set to 5 LUX at the maze level. Mice were placed in the enclosed quadrant and were allowed to explore for 5 min. Sessions were video recorded using a camera mounted above the apparatus which was connected to an outside computer allowing the experimenter to exit the room as soon as the mouse was placed in the apparatus. Latency to enter the open quadrant, time spent in open and closed quadrants, as well as number of quadrant entries were analyzed using Odor (Macropod Software, Yarraville, Australia).

Audiogenic seizures—Audiogenic seizures were performed as described previously (Gross et al., 2015b). P26-P28 day old mice were tested with two mice per cage between 7 and 8 pm. Before the actual testing, mice were habituated in the testing chamber and the environment for 30 minutes. A personal alarm (120dB attached with an A/C power adaptor and installed inside the testing cage) was used for the sound induction. The alarm sound was played twice for two minutes with a one-minute silence interval. Sound-induced behaviors such as wild running or a full tonic-clonic convulsion were recorded.

Prepulse inhibition—To assess sensorimotor gating, prepulse inhibition testing of the acoustic startle response was performed as described in (Schaefer et al., 2009). Briefly, mice were singly placed in a sound-attenuated chamber (SR Laboratory, San Diego Instruments, CA) inside a cylindrical acrylic holder with sliding door at each end mounted on a platform. A piezoelectric force transducer was mounted beneath the platform to record movement of mice. Background white noise was set at 55 dB. Mice were placed in the cylindrical test chamber for a 5 min acclimatization period followed by four types of 4×4 Latin square sequences of trials (zero stimulus, startle stimulus alone, 59 dB prepulse + startle stimulus, 70 dB prepulse + startle stimulus, or 80 dB prepulse + startle stimulus), repeated three times for a total of 48 trials. The intertrial interval and interstimulus interval from prepulse onset to startle signal onset was 8 sec and 70 ms, respectively. The startle signal was 120 dB which lasted 0.2 s.

Contextual conditioned freezing—The mice were tested as per the protocol by (Kuerbitz et al., 2018) with modifications. The apparatus consisted of an acrylic chamber (25 × 25 cm, Freeze Monitor System; San Diego Instruments, CA) equipped with a 16 × 16 photo beam array, ceiling light and speaker, and had metal grid floors connected to a foot

shock source. On day 1, mice were placed in the chamber for 12 min consisting of 6 min of acclimation without stimulus followed by 6 min with nine tone-shock pairings (82 dB for 30 s paired with a 2 s long 1 mA foot shock during the last second of the 30 s tone interval). Day 2 consisted of 6 min exploration period in the same chamber without shock or stimulus to assess contextual memory. On day 3, mice were placed in a different environment (black, triangular box with black lid with light, 50% smaller than the conditioning chamber). A 3 min no-tone interval was followed by ten 30 s periods of alternating tone and silence to test cued memory and extinction. Day 4 was similar to day 3 except only 5 alternating periods of tone silence were used to measure cued recall. The number of photo beam breaks while in the chamber was used as a measurement of activity versus freezing.

Electrode implantation and electroencephalography

6–8 week-old male Kv4.2^{HET} mice and littermate WT controls were implanted with wireless transmitters for EEG monitoring (Castro et al 2012). The mice were first anesthetized with 4% isoflurane in medical grade oxygen in a closed chamber, and then maintained at 0.7–1.5% isoflurane throughout the surgery and monitored for adequate respiration patterns. Single channel wireless EEG transmitters (TA11ETA-F10, Data Science International (DSI), St. Paul, MN) were used. The head was first shaved and disinfected using Dermachlor (2% Chlorhexidine), and carprofen (100 μl) was administered subcutaneously. The skull was exposed by making an incision along the midline. Dorsoventral coordinates were measured from bregma and two holes were drilled at AP = −2.5 mm, L = ± 2.0 mm (Tse et al., 2014). Approximately 1 mm length of each of the two leads of the transmitter was inserted into the burr holes on top of the dura and sealed using GLUture (Zoetis Inc., Kalamazoo, MI). The wireless transmitter was placed subcutaneously by creating a pocket behind the neck. A screw was attached to the back of the skull and dental cement (Lang Dental, IL) applied to secure the assembly. After the cement had dried, the incision was closed using surgical sutures (Coviden, Dublin, Ireland) and sealed with GLUture (Abbott Laboratories). Post-surgery, the mice were injected with 1 ml saline, placed on a heating pad, and monitored during recovery.

Video-EEG recording and spectral power analysis

Post-recovery, the mice were housed in individual cages placed on wireless receiver plates (RPC1; DSI). DATAQUEST A.R.T software was used for recording EEG data received from the telemetry system sampled at 500 Hz, which provided readouts for frequencies between 1 and 200 Hz (maximal sampling rate of the wireless transmitter TA11ETA-F10). Video was continuously recorded (Axis 221, Axis communication) in parallel and synchronized with the EEG signal. Video-EEG data were recorded for up to 4 weeks. The EEG recording data were analyzed using NeuroScore software (DSI). For EEG power analyses, the raw EEG signal was exported in 10 s epochs and subjected to Fast Fourier Transformation to generate power bands. A 5 min period of recording (free of any grooming behavior to avoid grooming-associated artifacts) was selected from individual mice from 2-h intervals during the day and night period (12pm to 2pm and 12am to 2am, respectively, with very few exceptions for which the hours of analysis were extended to 11am-3pm or 11pm-3am because of excessive signal artifacts, movement or grooming during the 12–2pm/am periods). These time periods were selected as there was minimum traffic of other

experimenting personnel in the room. The EEG signal was split into power bands of the following frequencies: delta (δ, 0.5–4 Hz), theta (θ, 4–8 Hz), alpha (α, 8–12 Hz), sigma (Σ, 12–16 Hz), beta (β, 16–24 Hz) and gamma (γ, 24–80 Hz) (Tse et al., 2014). These individual power bands were compared between the Kv4.2^{HET} and WT mice. The data were pooled from 10 s epochs for a total of 5 min duration. Mice with EKG signal or highly noisy EEG were removed from analysis (10 mice per genotype were implanted and 4 from each group were excluded).

Spike analysis

EEG spikes were detected using a spike detector module in NeuroScore™ version 3.2.1 (EEG analysis software). A spike was defined as having a duration of 1 – 70 ms and an absolute amplitude value of 150 μV – 1500 μV (Puttachary et al., 2015). Spike trains were defined as having a minimum duration of 5 ms with a minimum of 4 spikes spaced within 80–5000 ms apart from one another (Puttachary et al., 2015; Losing et al., 2017). EEG artifacts due to movement or grooming (identified by the video recordings) were manually removed. As described for the power analyses, mice with EKG signal or highly noisy EEG were removed from analysis (10 mice per genotype were implanted and 4 from each group were excluded). Data were analyzed in the same 2-h periods as described for EEG power analysis above.

Kainic acid seizure model

6–8 week-old mice were implanted with transmitters for cortical surface EEG telemetry recording as above. Post-surgery, the mice were allowed to recover for 24h and baseline EEG was recorded for 15–20 min, followed by intraperitoneal (i.p.) injection with kainic acid (2 mg/ml solution in sterile Ringers, 15 mg/kg body weight). Mice were returned immediately to the recording platform to measure seizure onset and EEG power. EEG was recorded for 90 min, following which the seizures were terminated with a subcutaneous injection of diazepam (15 mg/kg).

In vitro assessment of lentivirus-mediated overexpression of Kv4.2 in HEK293 cells

HEK-293 cells (CRL-1573™, ATCC, Manassas, VA) were transfected at 80% confluency with increasing amounts of lentiviral (50,000–500,000 transfective units/ml). Cells were harvested after five days and analyzed by western blotting.

Intrahippocampal injection of lentivirus

Two different sets of experiments were performed using lentiviral overexpression of Kv4.2, aimed at measuring the effect of lentivirus injection on seizure susceptibility and the effect on Kv4.2 mRNA expression, respectively. The tissue from the seizure onset mice was not used for the biochemical quantification of Kv4.2, as kainic acid-induced seizure was shown to reduce the expression of Kv4.2 (Gross et al., 2016), and hence the specific effect of lentivirus overexpression would not have been measured accurately in those mice. To quantify *Kcnd2* mRNA levels, 6–8 week old C57/BL6 mice were subjected to bilateral intrahippocampal CA1 injections of *Kcnd2* expressing lentivirus or a negative control at bregma level AP = − 2.0 mm; L = ± 1.8 mm and V = 2.0 mm (2 μl/side= ~200,000

transfective units/side). Using a 5 μl Hamilton syringe, lentivirus was administered slowly over a 5 min duration and the needle was left in place for 10 min to allow the diffusion of the injected volume followed by a slow retraction of needle over a 5 min duration. Tissue was collected two weeks after virus injection. Before the experimental surgeries, the specificity of injection was confirmed using a dye injection. To assess seizure onset, mice were implanted with transmitters for EEG recording and at the same time received a bilateral intra-hippocampal injection of lentivirus overexpressing *Kcnd2* or a vector control at two different doses (1 μl/side= ~100,000 transfective units/side and 2 μl/side= ~200,000 transfective units/side). The transmitters were implanted as described above under "electrode implanting" followed by lentivirus injection as described above. Post injection, the incision was closed using surgical sutures, and GLUture and antibiotic ointment was applied. The mice were later administered with 1 ml of sterile Ringer's saline and placed on heating pad and monitored until recovery. Kainic acid-induced seizure onset and severity were analyzed two weeks after virus injection.

Image processing

Figures were prepared using Adobe Photoshop CS6 software. To enhance visibility, brightness and contrast of western blot images were adjusted equally across conditions using the "level" tool without changing midtone. Quantification was performed on the raw images using ImageJ (NIH).

Experimental design and statistical analysis

Non-behavioral data were analyzed using GraphPad Prism7 software. All data were analyzed for normality using the Shapiro-Wilk's test. For two-sample comparisons, appropriate parametric (unpaired two-sided t-test) or non-parametric tests (unpaired two-sided Mann Whitney test) were used as indicated in each figure legend. Dendritic spine morphology was analyzed by 2-way ANOVA (genotype × spine type as variables) followed by planned post-hoc comparisons of genotype-dependent differences for each spine type using Sidak's posthoc tests. Marble burying was analyzed by repeated measurements 2-way ANOVA (genotype and time as independent variables) followed by planned post-hoc comparisons of genotype-dependent differences for each time point using Sidak's tests. Statistical tests, sample sizes and p values are specified in the figure legends. Statistical significance was set to $\alpha < 0.05$. No mice were excluded from biochemical studies. Some mice were excluded from EEG power and spike/spike train analysis due to unusable signal as described in the respective method sections. Data are represented as scattered plots with bars and error bars indicating mean ± SEM, except for EEG power, spikes and spike trains, which are presented as box-and-whisker plots which show minimum to maximum (whiskers), 25^{th} to 75^{th} percentile (boxes) and median (line). Behavioral data were analyzed using mixed linear model ANOVAs (Proc Mixed, SAS v9.4, SAS Institute, Cary, NC). The autoregressive moving average (ARMA) variance-covariance model was used in conjunction with Kenward-Roger first order degrees of freedom. Significant interactions were analyzed using slice-effect ANOVAs. For PPI of the startle response, separate analyses were done for each day since Proc Mixed is unable to handle two repeated measures involving time.

Where applicable, statistical power was calculated using free online sample size and power calculators (powerandsamplesize.com). Sample sizes were determined as follows: We expected to detect a reduction in Kv4.2 protein or mRNA by half in Kv4.2 heterozygous with the commonly observed 30% variability in western blot and qRT-PCR. The required sample size for statistical power of 0.8 was determined as n=10. We previously observed that a sample size of 23–27 was needed for detecting a difference in dendritic spine density of 0.96/1.133 with a standard deviation of 0.23 yielding a statistical power of 0.76 (Gross et al., 2019). After reaching a sample size of ~27 in the analysis of Kv4.2 heterozygous and wildtype mice, we performed power analyses of the data and determined a sufficient statistical power of p=0.9995. Here, male and female mice were analyzed together (3 male mice per genotype, 3 female WT and 2 female Kv4.2^{HET} mice). Sample sizes for behavioral experiments were based on previous data (Schaefer et al., 2009). As no trends or differences were determined with ~20 mice or 12 mice per group, no further power analyses were performed. Startle response and conditioned freezing were performed in 12 cohorts with one mouse per genotype per litter, reducing litter effects, whereas on some occasions, multiple mice per genotype per litter were used for nesting and marble burying assays. Sample sizes were based on previous data (Gross et al., 2016). For quantification of western blots, seizure onset and EEG power, analyzers were blind to the condition. For behavioral assays and dendritic spine analyses, experimenters and analyzers were blind to the condition.

Results

Kv4.2 expression is reduced in Kv4.2^{HET} mice with no or only moderate effects on other subunits of the Kv4.2 channel complex

To confirm that genetic reduction of *Kcnd2* led to decreased mRNA and protein expression of Kv4.2, hippocampal tissue from Kv4.2^{HET} and WT littermates was assessed by western blot and quantitative real-time PCR. Kv4.2 protein and mRNA levels were reduced to 50% or less in Kv4.2^{HET} mice compared with WT mice (Fig. 1A, B). By contrast, the closely related A-type channel Kv4.3, which is mainly expressed in the dentate gyrus and the hippocampal CA3 region, but virtually absent from the CA1 region where Kv4.2 is expressed (Alfaro-Ruiz et al., 2019), was unchanged (Fig. 1C). Localization and function of Kv4.2 channels are modulated by auxiliary subunits such as potassium channel interacting proteins (KChIPs) or dipeptidyl peptidase-like proteins (DPPs) (Nadal et al., 2003; Norris et al., 2010; Sun et al., 2011). To assess if genetic reduction of Kv4.2 alters the expression of these auxiliary subunits, we analyzed hippocampal tissue of Kv4.2^{HET} mice and WT littermates by western blot specific for different KChIPs and DPPs. A moderate reduction in the level of KChIP3 protein was observed (~30%, Fig. 1D, F) whereas mRNA levels were unchanged (*not shown*). None of the other auxiliary subunits tested (DPP6, DPP10 and KChIP2) changed (Fig. 1E–I). These results confirm that Kv4.2 heterozygous mice are a model for reduced Kv4.2 expression and suggest that reduction of Kv4.2 has limited effects on expression levels of auxiliary subunits.

Kv4.2^{HET} mice have reduced dendritic spine density and altered dendritic morphology in the hippocampus

Kv4.2 protein is expressed in somata, dendrites, and dendritic spines of hippocampal CA1 pyramidal neurons (Kerti et al., 2012). The presence of Kv4.2 in dendrites and dendritic spines and its function in regulating dendritic excitability suggest that it may affect dendritic spine morphology; however, this has not been examined *in vivo*. Using fluorescent reporter mice and tissue clearing (Fig. 2A), we showed that dendritic spine density of hippocampal CA1 pyramidal neurons was reduced in Kv4.2^{HET} mice compared with littermate controls (Fig. 2B, C). Dendritic spine morphology analysis demonstrated a significant reduction in mushroom-shaped spines and an increase in filopodia-like and thin spines in Kv4.2^{HET} mice compared with control (Fig 2D). No significant changes in the proportion of stubby spines was observed (Fig 2D). Similar trends of reduced dendritic spine density were observed in male (Fig. 2E) and female (Fig. 2F) mice, suggesting that Kv4.2 reduction affects dendritic spine density independently of sex. Overall, these findings suggest that reduced expression of Kv4.2 leads to lower numbers of dendritic spines in the hippocampal CA1 network with a more immature morphology. Western blot analyses of tissue slices confirmed a similar reduction of Kv4.2 in this mouse model as described in Fig. 1 (Fig. S2).

Genetic reduction of Kv4.2 does not have an effect on overall anxiety levels or behavior

Alterations in dendritic spine morphology have been associated with behavioral abnormalities (Gipson and Olive, 2017). To investigate if altered dendritic spine morphology in Kv4.2^{HET} mice was associated with autism-related phenotypes, we next tested behaviors associated with anxiety, social function, and perseverative phenotypes. To rule out any adverse effects on behavior caused by differences in growth or body weight, we measured body weight every 2–3 days from postnatal week 3 to 7 in male and female Kv4.2^{HET} and WT mice. There was no difference between average weight of heterozygous and WT mice during this period (weight at 5 weeks of age: Het-male = 19.27 ± 1.9g, WT-male = 18.43 ± 2g, Het-female = 16.54 ± 2.1g and WT-female = 17.37 ± 1.2g).

Home cage social behavior was analyzed by nesting behavior. We detected no difference in nesting between male or female Kv4.2^{HET} and WT mice by nesting score (Deacon, 2006) and the percentage of nestlet torn 2 h and 24 h after adding fresh nestlet to the cage (Fig. 3A, B, *nesting scores from male mice shown*).

To assess perseverative or repetitive behavior, a core feature of autism, we analyzed if genetic reduction of Kv4.2 led to changes in marble burying behavior (Thomas et al., 2009). No difference in the latency to start burying marbles (Fig. 3C) or the number of marbles buried at different time points during the test (5 min, 10 min and 15 min) was observed (Fig 3D) indicating no increase in repetitive behavior in male or female Kv4.2^{HET} mice (*only data in male mice are shown*). To evaluate whether reduced Kv4.2 expression has any effects on anxiety-like behavior we tested mice in an elevated zero maze. Time spent in open or closed quadrants is a measure of anxiety-related behavior (Walf and Frye, 2007). No difference in the latency to open quadrant entry (Fig. 3E), the time spent in the open quadrants (Fig. 3F) or transitions between the open and closed quadrants (Fig. 3G) of the maze was observed. Similarly, no difference in the number of head dips was observed (*data*

not shown). These results show that reduced Kv4.2 does not affect anxiety-like or perseverative behavior, suggesting that reduced Kv4.2 *per se* does not induce autistic-related behavior.

Kv4.2^{HET} mice show normal sensorimotor gating behavior

Impaired sensorimotor gating has been observed in individuals with autism as well as in autism mouse models (Perry et al., 2007; Sinclair et al., 2017). To evaluate potential autistic-like phenotypes in Kv4.2^{HET} mice, we next tested sensorimotor gating using a prepulse inhibition (PPI) of acoustic startle response paradigm. The peak amplitude of the startle response with or without prepulse was recorded on two consecutive days. We observed no difference in the overall acoustic startle response or in the response inhibition after three different acoustic prepulses between Kv4.2^{HET} mice and their WT littermates during two days of testing (Fig. 3H, I). These results suggest that acoustic startle and sensorimotor gating are normal in Kv4.2^{HET} mice. To further assess the response to acoustic stimulation we also tested if Kv4.2^{HET} mice were prone to audiogenic seizures. Two of 23 Kv4.2^{HET} mice experienced a seizure upon a 120dB sound stimulation, whereas none of the 13 WT littermates seized (two-sided Fisher's exact test: p=0.525). The two mice that seized came from the same litter, and we observed a similar rate of ~10% audiogenic seizures in C57BL/6J WT control mice from our breeding colony in previous studies (Gross et al., 2015b; Gross et al., 2015a). We therefore conclude that Kv4.2^{HET} mice are not prone to audiogenic seizures.

Kv4.2^{HET} mice exhibit normal contextual and cued conditioned freezing memory

Kv4.2^{HET} mice have altered dendritic spine morphology in the hippocampal CA1 region, suggesting defective hippocampal function that could affect learning and memory. In a previous study by Lugo et al, Kv4.2^{KO} mice showed impaired contextual learning during a conditioned freezing test but no difference in cued freezing (Lugo et al., 2012). To analyze the effect of reduced Kv4.2 levels on conditioned learning, mice were tested for contextual and cued freezing. During the conditioning phase, both the Kv4.2^{HET} mice and WT littermate controls showed the same level of activity as measured by the number of beam breaks while in the chamber (Fig. 3J). On the following day mice were tested for contextual memory (without tone or shock), which showed the expected reduction in behavior in both genotypes (Fig. 3K). Similarly, activity reductions were the same in the two genotypes when presented with the tone in a new environment (cued memory) (Fig. 3L) and during the recall phase to test extinction memory (Fig. 3M). These results indicate that reduced Kv4.2 expression does not affect conditioned freezing memory in mice.

Genetic reduction of Kv4.2 increases basal EEG theta power and spike frequency

Brain electrographic characteristics such as irregular EEG power of specific frequency bands and epileptiform spikes signify an hyperexcitable or epileptogenic network and have been observed in both pharmacologically induced (Tse et al., 2014) and genetic mouse models of epilepsy (Dhamne et al., 2017). To assess if reduction in Kv4.2 leads to a hyperexcitable network, we analyzed baseline EEG power spectrum characteristics by quantifying different frequency bands of cortical EEG signal in freely behaving mice. In addition, we assessed the average frequency of spikes and spike trains (example traces shown in Fig. 4A and Fig. S3).

We chose cortical surface EEG recording to avoid potential side effects of intracranial electrodes due to tissue scarring or inflammation. We observed a significant increase in θ power (Fig. 4B, H) and a trend towards increased α power (Fig. 4C, I) in cortical surface EEG recordings from Kv4.2^{HET} mice compared with WT control during both the day and night period. No significant differences in other waveforms were detected during the day (Fig. 4D–G) or the night period (Fig. 4J–M). Spike analysis showed an overall non-significant increase in the number of spikes (Fig. 4N, P) and spike trains (Fig. 4O, Q) in the Kv4.2^{HET} mice during the day and night period. These results suggest an abnormal neuronal network and increased baseline excitability in Kv4.2^{HET} mice.

Genetic reduction of Kv4.2 reduces latency to seizure onset and increases seizure-induced EEG power in a mouse model of *status epilepticus*

Reduced expression of Kv4.2 has been observed in several mouse models of epilepsy, but it is unknown if reduced Kv4.2 by itself causes a hyperexcitable network. To address this question, we investigated the effect of reduced Kv4.2 on seizure susceptibility using the acute kainic acid model of *status epilepticus.* Mice were implanted with cortical surface electrodes for continuous video-EEG monitoring. After a 3-day recovery period, baseline EEG was recorded for 20 min followed by intraperitoneal kainic acid injection to induce *status epilepticus* (timeline shown in Fig. 5A). A significant decrease in the latency to seizure onset was observed in Kv4.2^{HET} mice compared with WT controls (Fig. 5B). Moreover, Kv4.2^{HET} mice showed a significant increase in theta power compared with WT controls after kainic acid (Fig. 5C). No effect was observed on α, δ, Σ and β power, although these increases approached significance (Fig 5D–G). These results are consistent with the notion that reduced levels of Kv4.2 lead to a hyperexcitable neuronal network.

Lentivirus-mediated overexpression of Kv4.2 increases latency to seizure onset and reduces EEG power in a mouse model of *status epilepticus*

To further investigate the role of Kv4.2 in regulating brain excitability, we investigated the effect of hippocampal overexpression of Kv4.2 on seizure susceptibility in the kainic acid model of *status epilepticus*. We chose overexpression in WT and not Kv4.2^{HET} mice to avoid any potential compensatory effects caused by reduced KChIP3 in the Kv4.2^{HET} mice (Fig. 1D). This enabled us to assess the effect of increasing Kv4.2 levels in adult mice in isolation. We chose lentiviral vector-mediated overexpression for this approach as it offers a tool for rapid, stable and spatially restricted transgene expression (Lundberg et al., 2008). We first used an *in vitro* system to confirm that a lentivirus encoding the open reading frame of murine *Kcnd2* expressed Kv4.2 protein in mammalian cells (Fig. 6B). We then performed bilateral intrahippocampal CA1 injections of the Kv4.2-expressing lentiviral particles to overexpress Kv4.2 *in vivo* in mice. Lentiviral particles containing the empty vector served as a negative control. At the same time of viral injection, cortical surface EEG electrodes were implanted for EEG recording. Two weeks after viral injection, *status epilepticus* was induced by intraperitoneal injection of kainic acid as before, and latency to seizure onset and EEG power were analyzed by continuous video-EEG recording as described above (timeline shown in Fig. 6A). An initial dose of 1μl/side of lentiviral particles (100,000 transfective units) showed no significant effect on latency to seizure onset (Fig. 6C) or EEG power spectrum (data not shown) between the Kv4.2 expressing and the control mice; however,

injecting twice the amount of lentiviral particles (2μl/side) resulted in a significant increase in latency to seizure onset after Kv4.2 overexpression (Fig. 6D). Note that the latency to seizure onset was much shorter in the control mice than in the wildtype mice shown in Fig. 5B. We assume that the surgery and stereotaxic injection of lentiviral particles two weeks prior to the experiment increased the overall susceptibility to seizures despite the fact that mice recovered well and appeared overall healthy. Because Kv4.2- and control-injected mice were treated equally, we do not think that this affected the overall results showing delay of seizure onset with Kv4.2 overexpression. Evaluation of the EEG power spectrum showed a significant reduction of theta power in the Kv4.2-injected mice (Fig. 6E). No significant effect was observed on other waveforms (Fig. 6F–I). In a separate group of mice, we used qRT-PCR of hippocampal CA1 tissue punches to confirm that intrahippocampal CA1 injection of mice with Kv4.2-expressing lentiviral particles led to significantly increased Kv4.2 mRNA expression in the targeted region compared with mice injected with control lentiviral particles (Fig. 6J). Taken together, these results demonstrate the importance of Kv4.2 in regulating neuronal excitability.

Discussion

The etiology of autism and epilepsy is highly complex and diverse. Discovering pathological mechanisms that are shared and could be therapeutically targeted may be a promising strategy to identify broadly applicable novel therapies for these diseases. As a step towards this direction, we tested if reduced expression of the voltage-gated potassium channel Kv4.2, which is impaired in many rodent models of acquired or genetic epilepsy and autism, is a disease-causing factor underlying autistic-like behavior and brain hyperexcitability. Our studies showed that reduced Kv4.2 in mice leads to a hyperexcitable brain, as evident by increased frequency of electrographic spikes and increased susceptibility to kainic acid-induced seizures. Lentivirus-mediated overexpression of Kv4.2, by contrast, decreased seizure susceptibility and EEG power, corroborating that altered Kv4.2 levels may be a causal and targetable molecular phenotype underlying brain hyperexcitability in brain disorders. Mice with reduced Kv4.2 levels showed a decrease in dendritic spine density and an immature dendritic spine morphology in the hippocampus. These findings suggest more general impairments in brain function; however, they were not accompanied by changes in anxiety-like and perseverative behaviors, defects in sensorimotor gating, or conditioned freezing memory. In summary, our results suggest that Kv4.2 is an important regulator of neuronal excitability and brain network dynamics and therefore could be a treatment target in epilepsy.

Similarly as in a previous study in $Kv4.2^{KO}$ mice (Barnwell et al., 2009), we did not observe spontaneous seizures during four weeks of continuous video-EEG monitoring in 6–8 week-old $Kv4.2^{HET}$ mice. This suggests that reduced Kv4.2 levels do not lead to epilepsy in young adult mice; however, we only used cortical surface EEG recordings paired with video recordings and may have therefore missed focal hippocampal seizures. Despite the lack of spontaneous cortical seizures, we observed characteristics of a hyperactive brain network under baseline conditions. We detected on average increased numbers of spikes and spike trains in $Kv4.2^{HET}$ mice compared with WT littermates. Individual waveform characterization of electrographic power spectra also revealed that $Kv4.2^{HET}$ mice have

significantly increased theta power compared with WT littermates. EEG abnormalities are characteristic features of autism and epilepsy and are observed in both patients and animal models (Keller et al., 2017). Changes in theta activity, for example, were shown to be associated with seizure occurrence in five different mouse models (Milikovsky et al., 2017), and interictal epileptiform spikes may predict epilepsy (White et al., 2010) and correlate with epilepsy severity (Rosati et al., 2003). Kv4.2^{HET} mice showed a trend towards increased epileptiform spike frequency and significantly elevated theta power at a relatively young age. It is possible that the hyperexcitable phenotype in Kv4.2^{HET} mice may worsen over time. Future studies are needed to assess if spontaneous recurrent seizures occur in aged Kv4.2^{HET} mice. Here, we focused on the effect of life-long reduction of Kv4.2 on brain excitability. Life-long reduction of Kv4.2 most likely mimics genetic epilepsy and autism disorders that have reduced Kv4.2 expression or function over the life span. Future studies are needed to assess if acute down-regulation of Kv4.2 as observed in acquired epilepsies, e.g. after traumatic brain injury or *status epilepticus*, leads to epileptogenesis and the development of spontaneous recurrent seizures in mice. A limitation of this study is that we were not able to reliably discern immobile wake from sleep phases for the EEG analysis. As brain activity changes with wake or sleep stages, this might have skewed the data, and more detailed follow-up studies are needed to test the effect of sleep cycles on brain activity in Kv4.2 heterozygous mice.

Apart from showing that reduction in Kv4.2 levels increases the susceptibility to seizures, we also observed that bilateral intrahippocampal CA1 injections of a lentivirus overexpressing Kv4.2 delayed seizure onset and reduced EEG power. These findings suggest a bidirectional role of Kv4.2 in modulating seizure susceptibility. Increasing Kv4.2 levels using microRNA manipulation (Tiwari et al., 2019) or viral strategies (present study) could thus represent a novel therapeutic strategy for epilepsy. A recent study in mice supported the therapeutic benefit of overexpressing potassium channels as a gene therapy in epilepsy (Snowball et al., 2019). Further investigation is needed to confirm the potential seizure delaying effect of viral overexpression of Kv4.2 using different mouse models of *status epilepticus* and acquired or genetic epilepsy. Nevertheless, our results show that virus-mediated overexpression of Kv4.2 may be a useful tool to modulate network excitability and seizures.

Consistent with the observed changes in basal brain activity and function, we detected altered dendritic spine morphology in Kv4.2^{HET} mice. In particular, we observed reduced dendritic spine density and an immature appearance of spines, i.e. less mushroom-type spines and more thin and filopodia-type spines. This suggests that Kv4.2 is important for dendritic spine maturation, which is supported by a study that showed impaired molecular maturation of Kv4.2^{KO} synapses on apical dendrites of CA1 pyramidal neurons (Kim and Hoffman, 2012). Alterations in dendritic spine density and morphology are a characteristic neuropathological feature of autism and epilepsy (Peebles et al., 2010; Martinez-Cerdeno, 2017). While often times, increased excitability is associated with increased dendritic spine density, there are a few epilepsy disorders, for example Rett syndrome and Tuberous sclerosis complex (TSC) that were shown to have reduced dendritic spine density similarly as reported here (Huttenlocher and Heydemann, 1984; Tavazoie et al., 2005; Belichenko et al., 2009). Reduction in dendritic spine density could be a compensatory mechanism in

response to excessive excitability in the dendrite. Another, maybe more likely explanation is that changes in the numbers of dendritic spines will lead to complex circuit alterations, which could cause the observed brain excitability. Alternatively, rather the change in proportion of spine types than the absolute number of dendritic spines may drive the increased susceptibility to seizures in this mouse model by changing brain circuits (Wong and Guo, 2013). Our findings of immature dendritic spine morphology in Kv4.2^{HET} mice are thus consistent with the hypothesis that reduced Kv4.2 contributes to epileptic phenotypes and potentially other brain dysfunctions. We detected ~1 spine per μm in CA1 apical dendrites of WT mice, which is in line with what we and others reported previously in fixed tissue (Perez-Cruz et al., 2011; Bhattacharya et al., 2012; Gross et al., 2019), but may underestimate the actual density due to limited optical resolution (Attardo et al., 2015). We cannot exclude that this potential underestimation may cause a bias in the spine types detected but assume that it would have affected both genotypes equally and is thus not invalidating our results.

In addition to dendritic spine density and morphology playing a role in autism and epilepsy, theta oscillations may influence memory, emotions and cognition (Korotkova et al., 2018). The alterations in EEG and dendritic spines caused by reduced Kv4.2 levels thus suggest that brain function is impaired in Kv4.2^{HET} mice; however, we did not detect deficits in behavioral and cognitive assays. The behavioral paradigms performed were limited in number and specifically chosen to test for broad autism- and hyperexcitability-associated phenotypes, such as anxiety (elevated zero maze), home cage behavior (nesting), perseverative behavior (marble burying), memory (conditioned freezing), and sensorimotor gating (prepulse inhibition). The observed changes in theta oscillations and dendritic spine morphology may not be sufficient to cause alterations in these behaviors and brain functions. This is in contrast to Kv4.2^{KO} mice that likewise do not display anxiety-related behaviors but showed impaired learning in contextual conditioned freezing (Lugo et al., 2012), and suggests that residual levels of Kv4.2 are sufficient for normal conditioned freezing. In summary, our behavioral analyses do not support a causal relationship between reduced Kv4.2 expression and autistic-like phenotypes. Previous work suggested that a mutation in *KCND2* that leads to functional changes in closed-state inactivation causes autism and seizures (Lee et al., 2014; Lin et al., 2018). Future investigations could assess if similar mutations in *KCND2* are common in autism spectrum disorders. Notably, reduced Kv4.2 has been reported in a mouse model of Alzheimer's disease, where it may contribute to increased susceptibility to seizures and cognitive impairments (Hall et al., 2015). Future studies are needed to perform a more thorough analysis of cognition, e.g. by testing spatial navigation or decision making, to further evaluate brain function in Kv4.2 heterozygous mice and test if they could serve as a mouse model of Alzheimer's disease.

A limitation of this study is that, apart from a decrease in Kv4.2, we also detected significantly reduced levels of the accessory protein KChIP3 in Kv4.2^{HET} mice. Kv4 channels are multiprotein complexes containing principal and auxiliary subunits (Vacher and Trimmer, 2011). Dipeptidyl peptidases (DPPs) and potassium channel interacting proteins (KChIPs) are the two main classes of auxiliary subunits known to interact with the Kv4.2 channel (Rhodes et al., 2004; Kim et al., 2008), and KChIP subunits were shown to regulate the surface expression of the complex (Shibata et al., 2003). Studies in KChIP3 knockout

mice have suggested that loss of KChIP3 reduces A-type current densities (Norris et al., 2010; Norris and Nerbonne, 2010); hence, the observed downregulation of KChIP3 might have potentiated the loss of Kv4.2 expression in this model. Of note, KChIP3 was shown to be reduced in the hippocampus of mice following kainic acid-induced seizure and in patients with epilepsy (Hong et al., 2003) further supporting the validity of $Kv4.2^{HET}$ mice as a model of a shared molecular phenotype in epilepsy. By contrast, no changes in the expression of other subunits (DPP6, DPP10 and KChIP2) or, importantly, Kv4.3, another A-type potassium channel that is expressed and functional in the hippocampus (Serodio and Rudy, 1998; Alfaro-Ruiz et al., 2019) were detected. This suggested lack of other potential compensatory mechanisms affecting A-type currents in the hippocampus; however, western blot analysis is semiquantitative, and we thus might have missed subtle changes in expression levels of other Kv4 channel complex subunits that could affect Kv4 channel function. Moreover, observed percentages of reduction might have not been entirely accurate.

In summary, this study shows that Kv4.2 expression is a critical determinant of neuronal network excitability in the brain. This has two important implications: first, it provides support for a causal role of reduced Kv4.2 in mouse models of epilepsy; and second, it suggests that increasing Kv4.2 levels may be seizure-suppressive and thus therapeutic in epilepsy. Our study does not directly support a role of impaired Kv4.2 in mediating autistic-like behavior or cognitive deficits in mice. However, the fact that basal brain function is altered in $Kv4.2^{HET}$ mice (dendritic spine morphology and theta oscillations) indicates that cognition or behavior may also be deficient. The present study mainly focused on the hyperexcitability phenotype. Future studies are necessary to further analyze a potential causal role of Kv4.2 in autism, including more sophisticated behavioral analyses over a wider age-range.

Supplementary Material

Refer to Web version on PubMed Central for supplementary material.

Acknowledgements:

This research work was supported by a postdoctoral fellowship from the American Epilepsy Society (grant number #506835) (DT), a Trustee Award by the Cincinnati Children's Research Foundation (CG), and the National Institutes of Health (1R01NS092705 and an Institutional Clinical and Translational Science Award, NIH/NCRR Grant Number UL1TR001425) (CG). The content is solely the responsibility of the authors and does not necessarily represent the official views of the NIH. The authors thank Dr. Jeanne Nerbonne for providing the Kv4.2 KO mice, Chiho Sugimoto for technical assistance, Angela White for preparing the graphical abstract, and Dr. Kenny Campbell as well as all members of the Gross and Danzer labs for helpful discussions.

References

Alfaro-Ruiz R, Aguado C, Martin-Belmonte A, Moreno-Martinez AE, Lujan R (2019) Expression, Cellular and Subcellular Localisation of Kv4.2 and Kv4.3 Channels in the Rodent Hippocampus. International journal of molecular sciences 20.

Andrasfalvy BK, Makara JK, Johnston D, Magee JC (2008) Altered synaptic and non-synaptic properties of CA1 pyramidal neurons in Kv4.2 knockout mice. J Physiol 586:3881–3892. [PubMed: 18566000]

Attardo A, Fitzgerald JE, Schnitzer MJ (2015) Impermanence of dendritic spines in live adult CA1 hippocampus. Nature 523:592–596. [PubMed: 26098371]

Barnwell LF, Lugo JN, Lee WL, Willis SE, Gertz SJ, Hrachovy RA, Anderson AE (2009) Kv4.2 knockout mice demonstrate increased susceptibility to convulsant stimulation. Epilepsia 50:1741–1751. [PubMed: 19453702]

Belichenko PV, Wright EE, Belichenko NP, Masliah E, Li HH, Mobley WC, Francke U (2009) Widespread changes in dendritic and axonal morphology in Mecp2-mutant mouse models of rett syndrome: Evidence for disruption of neuronal networks. Journal of Comparative Neurology 514:240–258. [PubMed: 19296534]

Bernard C, Anderson A, Becker A, Poolos NP, Beck H, Johnston D (2004) Acquired dendritic channelopathy in temporal lobe epilepsy. Science 305:532–535. [PubMed: 15273397]

Bhattacharya A, Kaphzan H, Alvarez-Dieppa AC, Murphy JP, Pierre P, Klann E (2012) Genetic removal of p70 S6 kinase 1 corrects molecular, synaptic, and behavioral phenotypes in fragile × syndrome mice. Neuron 76:325–337. [PubMed: 23083736]

Birnbaum SG, Varga AW, Yuan LL, Anderson AE, Sweatt JD, Schrader LA (2004) Structure and function of Kv4-family transient potassium channels. Physiol Rev 84:803–833. [PubMed: 15269337]

Casey JP et al. (2012) A novel approach of homozygous haplotype sharing identifies candidate genes in autism spectrum disorder. Hum Genet 131:565–579. [PubMed: 21996756]

Chen X, Yuan LL, Zhao C, Birnbaum SG, Frick A, Jung WE, Schwarz TL, Sweatt JD, Johnston D (2006) Deletion of Kv4.2 gene eliminates dendritic A-type K+ current and enhances induction of long-term potentiation in hippocampal CA1 pyramidal neurons. The Journal of neuroscience : the official journal of the Society for Neuroscience 26:12143–12151.

Connolly JJ, Glessner JT, Hakonarson H (2013) A genome-wide association study of autism incorporating autism diagnostic interview-revised, autism diagnostic observation schedule, and social responsiveness scale. Child development 84:17–33. [PubMed: 22935194]

Deacon RM (2006) Assessing nest building in mice. Nat Protoc 1:1117–1119. [PubMed: 17406392]

Dhamne SC, Silverman JL, Super CE, Lammers SHT, Hameed MQ, Modi ME, Copping NA, Pride MC, Smith DG, Rotenberg A, Crawley JN, Sahin M (2017) Replicable in vivo physiological and behavioral phenotypes of the Shank3B null mutant mouse model of autism. Molecular Autism 8:26. [PubMed: 28638591]

Dickstein DL, Dickstein DR, Janssen WGM, Hof PR, Glaser JR, Rodriguez A, O'Connor N, Angstman P, Tappan SJ (2016) Automatic Dendritic Spine Quantification from Confocal Data with Neurolucida 360. Current Protocols in Neuroscience 77:1.27.21–21.27.21. [PubMed: 27696360]

Francis J, Jugloff DG, Mingo NS, Wallace MC, Jones OT, Burnham WM, Eubanks JH (1997) Kainic acid-induced generalized seizures alter the regional hippocampal expression of the rat Kv4.2 potassium channel gene. Neurosci Lett 232:91–94. [PubMed: 9302094]

George Paxinos KF, George Paxinos, Keith Franklin (2012) The Mouse Brain in Stereotaxic Coordinates. Academic Press 4.

Gipson CD, Olive MF (2017) Structural and functional plasticity of dendritic spines - root or result of behavior? Genes Brain Behav 16:101–117. [PubMed: 27561549]

Gross C, Yao X, Pong DL, Jeromin A, Bassell GJ (2011) Fragile × mental retardation protein regulates protein expression and mRNA translation of the potassium channel Kv4.2. J Neurosci 31:5693–5698. [PubMed: 21490210]

Gross C, Raj N, Molinaro G, Allen AG, Whyte AJ, Gibson JR, Huber KM, Gourley SL, Bassell GJ (2015a) Selective Role of the Catalytic PI3K Subunit p110beta in Impaired Higher Order Cognition in Fragile × Syndrome. Cell reports 11:681–688. [PubMed: 25921527]

Gross C, Yao X, Engel T, Tiwari D, Xing L, Rowley S, Danielson SW, Thomas KT, Jimenez-Mateos EM, Schroeder LM, Pun RY, Danzer SC, Henshall DC, Bassell GJ (2016) MicroRNA-Mediated Downregulation of the Potassium Channel Kv4.2 Contributes to Seizure Onset. Cell reports 17:37–45. [PubMed: 27681419]

Gross C, Banerjee A, Tiwari D, Longo F, White AR, Allen AG, Schroeder-Carter LM, Krzeski JC, Elsayed NA, Puckett R, Klann E, Rivero RA, Gourley SL, Bassell GJ (2019) Isoform-selective

phosphoinositide 3-kinase inhibition ameliorates a broad range of fragile × syndrome-associated deficits in a mouse model. Neuropsychopharmacology 44:324–333. [PubMed: 30061744]

Gross C, Chang CW, Kelly SM, Bhattacharya A, McBride SM, Danielson SW, Jiang MQ, Chan CB, Ye K, Gibson JR, Klann E, Jongens TA, Moberg KH, Huber KM, Bassell GJ (2015b) Increased Expression of the PI3K Enhancer PIKE Mediates Deficits in Synaptic Plasticity and Behavior in Fragile × Syndrome. Cell reports 11:727–736. [PubMed: 25921541]

Guo W, Jung WE, Marionneau C, Aimond F, Xu H, Yamada KA, Schwarz TL, Demolombe S, Nerbonne JM (2005) Targeted deletion of Kv4.2 eliminates I(to,f) and results in electrical and molecular remodeling, with no evidence of ventricular hypertrophy or myocardial dysfunction. Circ Res 97:1342–1350. [PubMed: 16293790]

Guo Y, Baum LW, Sham PC, Wong V, Ng PW, Lui CHT, Sin NC, Tsoi TH, Tang CSM, Kwan JSH, Yip BHK, Xiao S-M, Thomas GN, Lau YL, Yang W, Cherny SS, Kwan P (2012) Two-stage genome-wide association study identifies variants in CAMSAP1L1 as susceptibility loci for epilepsy in Chinese. Human molecular genetics 21:1184–1189. [PubMed: 22116939]

Hall AM, Throesch BT, Buckingham SC, Markwardt SJ, Peng Y, Wang Q, Hoffman DA, Roberson ED (2015) Tau-dependent kv4.2 depletion and dendritic hyperexcitability in a mouse model of Alzheimer's disease. J Neurosci 35:6221–6230. [PubMed: 25878292]

Hong Y-M, Jo D-G, Lee M-C, Kim S-Y, Jung Y-K (2003) Reduced expression of calsenilin/DREAM/KChIP3 in the brains of kainic acid-induced seizure and epilepsy patients. Neuroscience Letters 340:33–36. [PubMed: 12648752]

Huttenlocher PR, Heydemann PT (1984) Fine structure of cortical tubers in tuberous sclerosis: A Golgi study. Annals of Neurology 16:595–602. [PubMed: 6508241]

Kalmbach BE, Johnston D, Brager DH (2015) Cell-Type Specific Channelopathies in the Prefrontal Cortex of the fmr1-/y Mouse Model of Fragile × Syndrome. eNeuro 2:ENEURO.0114–0115.2015.

Keller R, Basta R, Salerno L, Elia M (2017) Autism, epilepsy, and synaptopathies: a not rare association. Neurological sciences : official journal of the Italian Neurological Society and of the Italian Society of Clinical Neurophysiology 38:1353–1361.

Kerti K, Lorincz A, Nusser Z (2012) Unique somato-dendritic distribution pattern of Kv4.2 channels on hippocampal CA1 pyramidal cells. The European journal of neuroscience 35:66–75. [PubMed: 22098631]

Kim E, Hoffman DA (2012) Dynamic regulation of synaptic maturation state by voltage-gated A-type K+ channels in CA1 hippocampal pyramidal neurons. J Neurosci 32:14427–14432. [PubMed: 23055512]

Kim J, Nadal MS, Clemens AM, Baron M, Jung SC, Misumi Y, Rudy B, Hoffman DA (2008) Kv4 accessory protein DPPX (DPP6) is a critical regulator of membrane excitability in hippocampal CA1 pyramidal neurons. J Neurophysiol 100:1835–1847. [PubMed: 18667548]

Korotkova T, Ponomarenko A, Monaghan CK, Poulter SL, Cacucci F, Wills T, Hasselmo ME, Lever C (2018) Reconciling the different faces of hippocampal theta: The role of theta oscillations in cognitive, emotional and innate behaviors. Neuroscience & Biobehavioral Reviews 85:65–80.

Kuerbitz J, Arnett M, Ehrman S, Williams MT, Vorhees CV, Fisher SE, Garratt AN, Muglia LJ, Waclaw RR, Campbell K (2018) Loss of Intercalated Cells (ITCs) in the Mouse Amygdala of Tshz1 Mutants Correlates with Fear, Depression, and Social Interaction Phenotypes. J Neurosci 38:1160–1177. [PubMed: 29255003]

Lee H, Lin MC, Kornblum HI, Papazian DM, Nelson SF (2014) Exome sequencing identifies de novo gain of function missense mutation in KCND2 in identical twins with autism and seizures that slows potassium channel inactivation. Hum Mol Genet 23:3481–3489. [PubMed: 24501278]

Lee HY, Ge WP, Huang W, He Y, Wang GX, Rowson-Baldwin A, Smith SJ, Jan YN, Jan LY (2011) Bidirectional regulation of dendritic voltage-gated potassium channels by the fragile × mental retardation protein. Neuron 72:630–642. [PubMed: 22099464]

Lei Z, Deng P, Li J, Xu ZC (2012) Alterations of A-type potassium channels in hippocampal neurons after traumatic brain injury. Journal of neurotrauma 29:235–245. [PubMed: 21895522]

Lin MA, Cannon SC, Papazian DM (2018) Kv4.2 autism and epilepsy mutation enhances inactivation of closed channels but impairs access to inactivated state after opening. Proc Natl Acad Sci U S A 115:E3559–e3568. [PubMed: 29581270]

Losing P, Niturad CE, Harrer M, Reckendorf CMZ, Schatz T, Sinske D, Lerche H, Maljevic S, Knoll B (2017) SRF modulates seizure occurrence, activity induced gene transcription and hippocampal circuit reorganization in the mouse pilocarpine epilepsy model. Mol Brain 10:30. [PubMed: 28716058]

Lugo JN, Brewster AL, Spencer CM, Anderson AE (2012) Kv4.2 knockout mice have hippocampal-dependent learning and memory deficits. Learn Mem 19:182–189. [PubMed: 22505720]

Lugo JN, Smith GD, Arbuckle EP, White J, Holley AJ, Floruta CM, Ahmed N, Gomez MC, Okonkwo O (2014) Deletion of PTEN produces autism-like behavioral deficits and alterations in synaptic proteins. Front Mol Neurosci 7:27. [PubMed: 24795561]

Lundberg C, Bjorklund T, Carlsson T, Jakobsson J, Hantraye P, Deglon N, Kirik D (2008) Applications of lentiviral vectors for biology and gene therapy of neurological disorders. Current gene therapy 8:461–473. [PubMed: 19075629]

Martinez-Cerdeno V (2017) Dendrite and spine modifications in autism and related neurodevelopmental disorders in patients and animal models. Developmental neurobiology 77:393–404. [PubMed: 27390186]

Menegola M, Trimmer JS (2006) Unanticipated Region- and Cell-Specific Downregulation of Individual KChIP Auxiliary Subunit Isotypes in Kv4.2 Knock-Out Mouse Brain. The Journal of Neuroscience 26:12137–12142. [PubMed: 17122038]

Menegola M, Clark E, Trimmer JS (2012) The importance of immunohistochemical analyses in evaluating the phenotype of Kv channel knockout mice. Epilepsia 53 Suppl 1:142–149. [PubMed: 22612819]

Milikovsky DZ, Weissberg I, Kamintsky L, Lippmann K, Schefenbauer O, Frigerio F, Rizzi M, Sheintuch L, Zelig D, Ofer J, Vezzani A, Friedman A (2017) Electrocorticographic Dynamics as a Novel Biomarker in Five Models of Epileptogenesis. The Journal of neuroscience : the official journal of the Society for Neuroscience 37:4450–4461.

Monaghan MM, Menegola M, Vacher H, Rhodes KJ, Trimmer JS (2008) Altered expression and localization of hippocampal A-type potassium channel subunits in the pilocarpine-induced model of temporal lobe epilepsy. Neuroscience 156:550–562. [PubMed: 18727953]

Muddashetty RS, Kelic S, Gross C, Xu M, Bassell GJ (2007) Dysregulated metabotropic glutamate receptor-dependent translation of AMPA receptor and postsynaptic density-95 mRNAs at synapses in a mouse model of fragile × syndrome. J Neurosci 27:5338–5348. [PubMed: 17507556]

Nadal MS, Ozaita A, Amarillo Y, Vega-Saenz de Miera E, Ma Y, Mo W, Goldberg EM, Misumi Y, Ikehara Y, Neubert TA, Rudy B (2003) The CD26-related dipeptidyl aminopeptidase-like protein DPPX is a critical component of neuronal A-type K+ channels. Neuron 37:449–461. [PubMed: 12575952]

Norris AJ, Nerbonne JM (2010) Molecular dissection of I(A) in cortical pyramidal neurons reveals three distinct components encoded by Kv4.2, Kv4.3, and Kv1.4 alpha-subunits. J Neurosci 30:5092–5101. [PubMed: 20371829]

Norris AJ, Foeger NC, Nerbonne JM (2010) Interdependent Roles for Accessory KChIP2, KChIP3 and KChIP4 Subunits in the Generation of Kv4-encoded I(A) Channels in Cortical Pyramidal Neurons. The Journal of neuroscience : the official journal of the Society for Neuroscience 30:13644–13655.

Peebles CL, Yoo J, Thwin MT, Palop JJ, Noebels JL, Finkbeiner S (2010) Arc regulates spine morphology and maintains network stability in vivo. Proceedings of the National Academy of Sciences of the United States of America 107:18173–18178. [PubMed: 20921410]

Perez-Cruz C, Nolte MW, van Gaalen MM, Rustay NR, Termont A, Tanghe A, Kirchhoff F, Ebert U (2011) Reduced Spine Density in Specific Regions of CA1 Pyramidal Neurons in Two Transgenic Mouse Models of Alzheimer's Disease. The Journal of Neuroscience 31:3926–3934. [PubMed: 21389247]

Perry W, Minassian A, Lopez B, Maron L, Lincoln A (2007) Sensorimotor gating deficits in adults with autism. Biol Psychiatry 61:482–486. [PubMed: 16460695]

Puttachary S, Sharma S, Tse K, Beamer E, Sexton A, Crutison J, Thippeswamy T (2015) Immediate Epileptogenesis after Kainate-Induced Status Epilepticus in C57BL/6J Mice: Evidence from Long Term Continuous Video-EEG Telemetry. PLoS ONE 10:e0131705. [PubMed: 26161754]

Rhodes KJ, Carroll KI, Sung MA, Doliveira LC, Monaghan MM, Burke SL, Strassle BW, Buchwalder L, Menegola M, Cao J, An WF, Trimmer JS (2004) KChIPs and Kv4 alpha subunits as integral components of A-type potassium channels in mammalian brain. J Neurosci 24:7903–7915. [PubMed: 15356203]

Rodriguez A, Ehlenberger DB, Dickstein DL, Hof PR, Wearne SL (2008) Automated Three-Dimensional Detection and Shape Classification of Dendritic Spines from Fluorescence Microscopy Images. PLOS ONE 3:e1997. [PubMed: 18431482]

Rosati A, Aghakhani Y, Bernasconi A, Olivier A, Andermann F, Gotman J, Dubeau F (2003) Intractable temporal lobe epilepsy with rare spikes is less severe than with frequent spikes. Neurology 60:1290–1295. [PubMed: 12707431]

Routh BN, Johnston D, Brager DH (2013) Loss of functional A-type potassium channels in the dendrites of CA1 pyramidal neurons from a mouse model of fragile × syndrome. J Neurosci 33:19442–19450. [PubMed: 24336711]

Schaefer TL, Vorhees CV, Williams MT (2009) Mouse Pet-1 knock-out induced 5-HT disruption results in a lack of cognitive deficits and an anxiety phenotype complicated by hypoactivity and defensiveness. Neuroscience 164:1431–1443. [PubMed: 19786075]

Serodio P, Rudy B (1998) Differential expression of Kv4 K+ channel subunits mediating subthreshold transient K+ (A-type) currents in rat brain. J Neurophysiol 79:1081–1091. [PubMed: 9463463]

Shibata R, Misonou H, Campomanes CR, Anderson AE, Schrader LA, Doliveira LC, Carroll KI, Sweatt JD, Rhodes KJ, Trimmer JS (2003) A fundamental role for KChIPs in determining the molecular properties and trafficking of Kv4.2 potassium channels. J Biol Chem 278:36445–36454. [PubMed: 12829703]

Sinclair D, Oranje B, Razak KA, Siegel SJ, Schmid S (2017) Sensory processing in autism spectrum disorders and Fragile × syndrome-From the clinic to animal models. Neuroscience and biobehavioral reviews 76:235–253. [PubMed: 27235081]

Singh B, Ogiwara I, Kaneda M, Tokonami N, Mazaki E, Baba K, Matsuda K, Inoue Y, Yamakawa K (2006) A Kv4.2 truncation mutation in a patient with temporal lobe epilepsy. Neurobiol Dis 24:245–253. [PubMed: 16934482]

Snowball A, Chabrol E, Wykes RC, Shekh-Ahmad T, Cornford JH, Lieb A, Hughes MP, Massaro G, Rahim AA, Hashemi KS, Kullmann DM, Walker MC, Schorge S (2019) Epilepsy Gene Therapy Using an Engineered Potassium Channel. J Neurosci 39:3159–3169. [PubMed: 30755487]

Sun W, Maffie JK, Lin L, Petralia RS, Rudy B, Hoffman DA (2011) DPP6 establishes the A-type K(+) current gradient critical for the regulation of dendritic excitability in CA1 hippocampal neurons. Neuron 71:1102–1115. [PubMed: 21943606]

Tavazoie SF, Alvarez VA, Ridenour DA, Kwiatkowski DJ, Sabatini BL (2005) Regulation of neuronal morphology and function by the tumor suppressors Tsc1 and Tsc2. Nature Neuroscience 8:1727–1734. [PubMed: 16286931]

Thomas A, Burant A, Bui N, Graham D, Yuva-Paylor LA, Paylor R (2009) Marble burying reflects a repetitive and perseverative behavior more than novelty-induced anxiety. Psychopharmacology 204:361–373. [PubMed: 19189082]

Tiwari D, Brager DH, Rymer JK, Bunk AT, White AR, Elsayed NA, Krzeski JC, Snider A, Schroeder Carter LM, Danzer SC, Gross C (2019) MicroRNA inhibition upregulates hippocampal A-type potassium current and reduces seizure frequency in a mouse model of epilepsy. Neurobiol Dis:104508.

Tsaur ML, Sheng M, Lowenstein DH, Jan YN, Jan LY (1992) Differential expression of K+ channel mRNAs in the rat brain and down-regulation in the hippocampus following seizures. Neuron 8:1055–1067. [PubMed: 1610565]

Tse K, Puttachary S, Beamer E, Sills GJ, Thippeswamy T (2014) Advantages of Repeated Low Dose against Single High Dose of Kainate in C57BL/6J Mouse Model of Status Epilepticus: Behavioral and Electroencephalographic Studies. PLOS ONE 9:e96622. [PubMed: 24802808]

Vacher H, Trimmer JS (2011) Diverse roles for auxiliary subunits in phosphorylation-dependent regulation of mammalian brain voltage-gated potassium channels. Pflugers Archiv : European journal of physiology 462:631–643. [PubMed: 21822597]

Walf AA, Frye CA (2007) The use of the elevated plus maze as an assay of anxiety-related behavior in rodents. Nat Protoc 2:322–328. [PubMed: 17406592]

White A, Williams PA, Hellier JL, Clark S, Dudek FE, Staley KJ (2010) EEG spike activity precedes epilepsy after kainate-induced status epilepticus. Epilepsia 51:371–383. [PubMed: 19845739]

Wong M, Guo D (2013) Dendritic spine pathology in epilepsy: Cause or consequence? Neuroscience 251:141–150. [PubMed: 22522469]

Yang B, Treweek Jennifer B, Kulkarni Rajan P, Deverman Benjamin E, Chen C-K, Lubeck E, Shah S, Cai L, Gradinaru V (2014) Single-Cell Phenotyping within Transparent Intact Tissue through Whole-Body Clearing. Cell 158:945–958. [PubMed: 25088144]

Highlights

- Kv4.2 heterozygous mice have reduced dendritic spine density and altered morphology.
- Kv4.2 heterozygous mice do not display autistic-like or anxiety-related phenotypes.
- EEG analyses of Kv4.2 heterozygous mice suggest neuronal network hyperexcitability.
- Reduced Kv4.2 decreases latency to kainic acid-induced seizure onset.
- Lentiviral Kv4.2 overexpression increases latency to seizure onset.

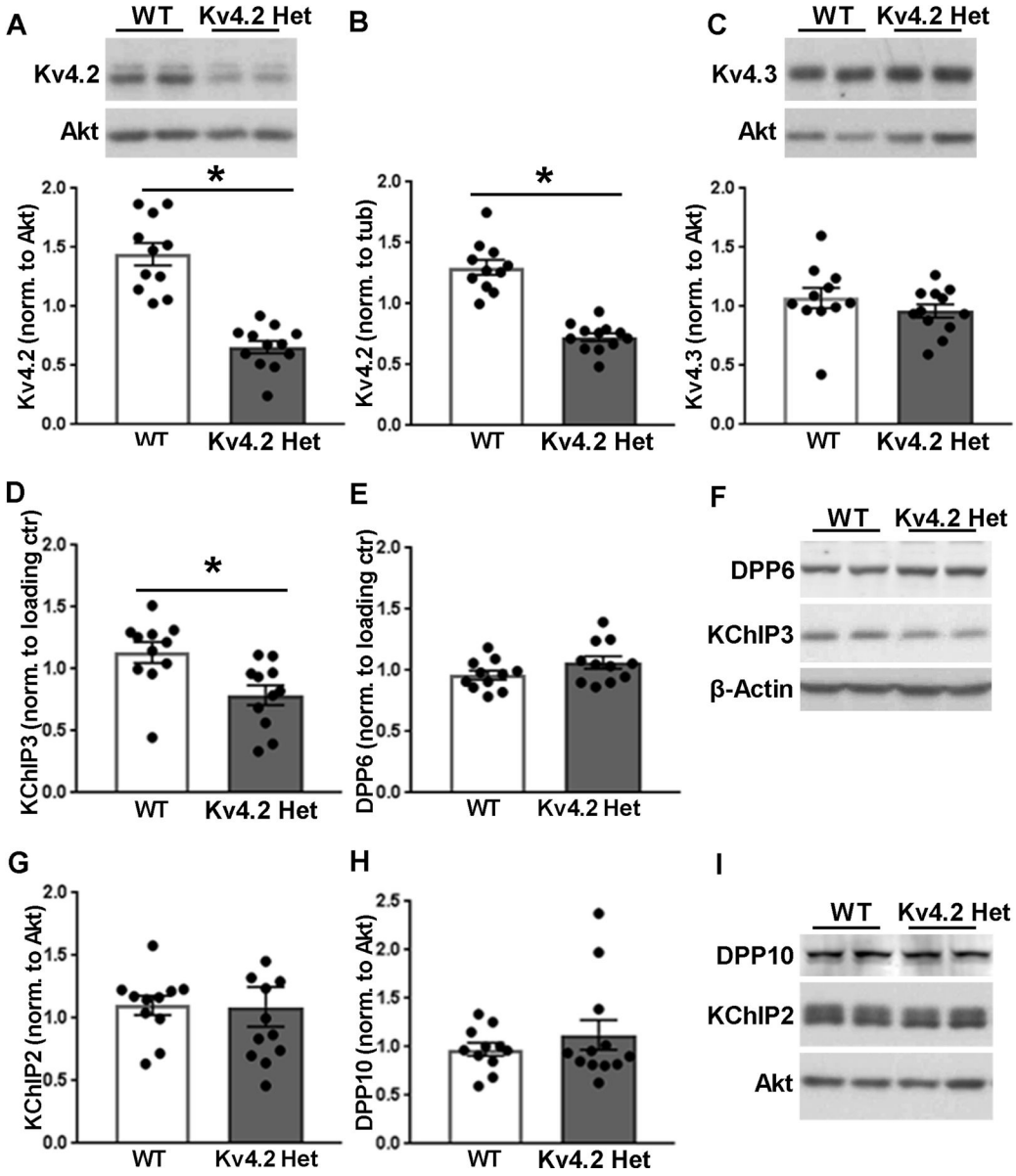

Figure 1: Kv4.2 and KChIP3 are reduced in Kv4.2 heterozygous mice.

(A, B) Kv4.2 protein (**A**) and mRNA levels (**B**) are significantly reduced in Kv4.2^{HET} mice compared with WT control (unpaired t-tests, WT: n=11, HET: n=12; **A**: t(21)=7.4, ***p<0.0001; **B**: t(21)=8.3, ***p<0.0001). **(C)** In contrast, Kv4.3 protein levels were unchanged (unpaired t-test, WT: n=11, HET: n=12; t(21)=1.1, p=0.286). **(D-I)** Of all tested auxiliary subunits of the Kv4.2 complex, only KChIP3 (**D,F**) was significantly reduced, whereas DPP6 (**E,F**), KChIP2 (**G,I**) and DPP10 (**H,I**) were unchanged (**D**: unpaired t-test, n=11, t(20)=2.97, p=0.008; **E**: unpaired t-test, n=11, t(20)=1.67, p=0.11; **G**: Mann Whitney test, WT: n=11, HET: n=12, p=0.83; **H**: Mann Whitney test, WT: n=11, HET: n=12, p=0.79). Example Western Blots are shown on top in **A** and **C**, as well as in **F** for **D** and **E**, and in **I** for **G** and **H**. An additional example of western blots shown in F is shown in Fig. S1A.

DPP6 and KChIP3 were either normalized to Akt or βActin, which did not differ between genotypes (Fig. S1B). Error bars represent SEM.

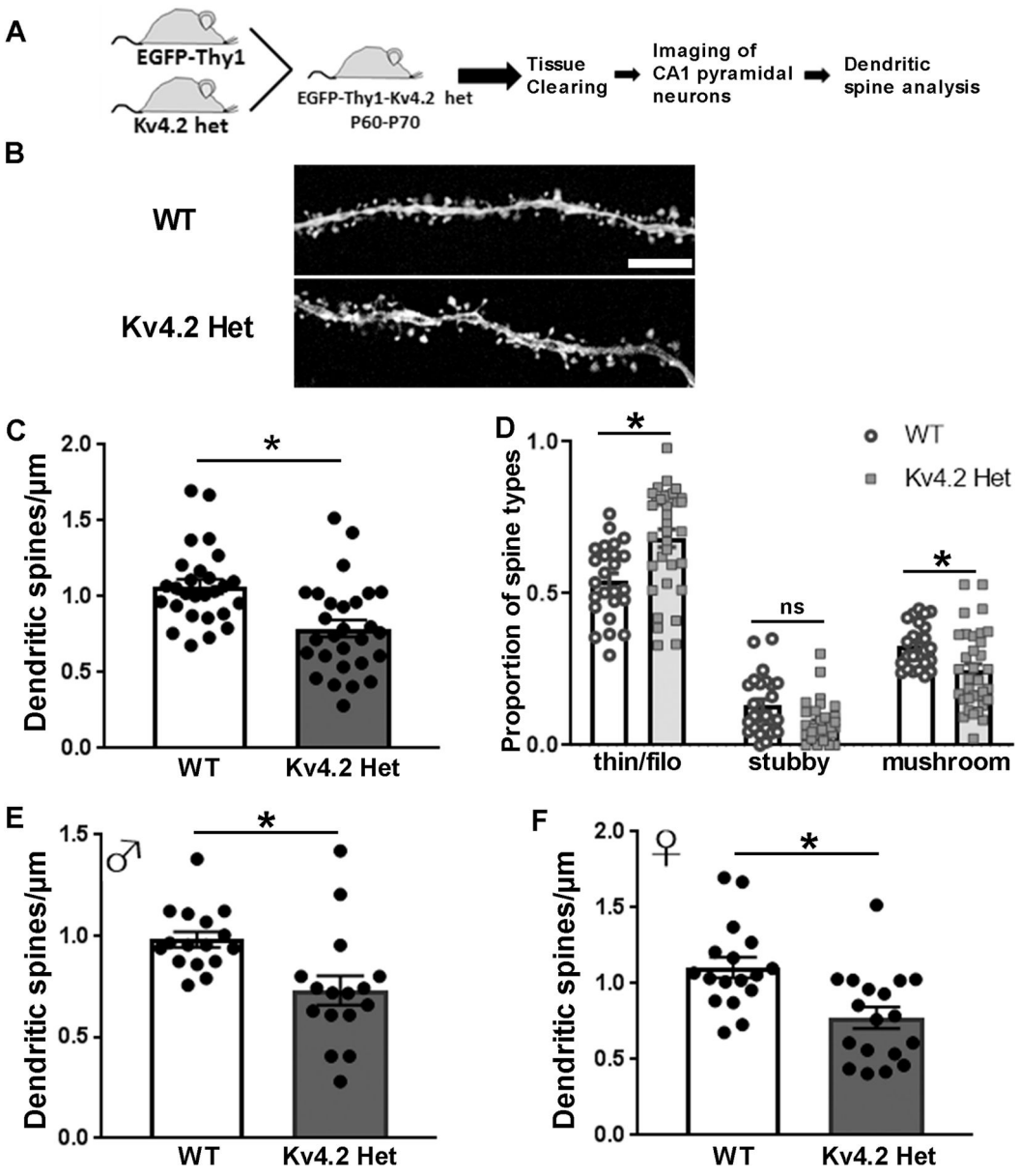

Figure 2: Kv4.2^{HET} mice have reduced dendritic spine density and immature dendritic spine morphology.

(A) Timeline depicting mouse breeding and steps involved in preparing the tissue for imaging and dendritic spine analysis. Neurons were visualized by transgenic expression of EGFP under a *thy1* promoter, tissue clearing and confocal imaging. **(B)** Representative images of dendrites from WT and Kv4.2^{HET} mice. Scale bar is 5 µm. **(C)** Dendritic spine density is reduced in 8–10 week-old Kv4.2^{HET} mice compared with WT littermates (WT: n=28 dendrites, 6 mice; HET: n=27 dendrites, 5 mice; unpaired t-test, t(53)=3.73; *p=0.0005). **(D)** The proportion of thin and filopodia-like dendritic spines is increased, whereas the proportion of mushroom-shaped dendritic spines is reduced in Kv4.2^{HET} mice (2-way ANOVA with Sidak's post hoc tests: interaction: F(2,171)=15.53, p<0.0001; spine type: F(2,171)=277, p<0.0001; genotype: F(1,171)<0.0001, p(genotype)>0.9999;

*p<0.0001, #p=0.030, p(ns)=0.156; n as in C). Mean+/−SEM: thin/filo WT: 0.542+/−0.025; thin/filo HET: 0.682+/−0.029; stubby WT: 0.132+/−0.019; stubby HET: 0.072+/−0.011; mushroom WT: 0.327+/−0.015; mushroom HET: 0.246+/−0.022. **(E,F)** Significant reduction in spine density was observed in male (E, WT: n=16 dendrites, 2 mice; HET: n=16, 3 mice, unpaired t-test, t(30)=3.10, *p=0.0042) and female mice (F, WT: n=17 dendrites, 3 mice; HET: n=18, 3 mice; unpaired t-test, t(33)=3.39, *p=0.0019). Dendritic spines were quantified using ImageJ (NIH) (**C,E,F**) and Neurolucida 360 (*MBF Bioscience*) (**D**). Error bars represent SEM. Reduction of Kv4.2 in *thy1*-EGFP Kv4.2 heterozygous hippocampus was similar as shown for mice without the *thy1*-EGFP transgene (Fig. S2).

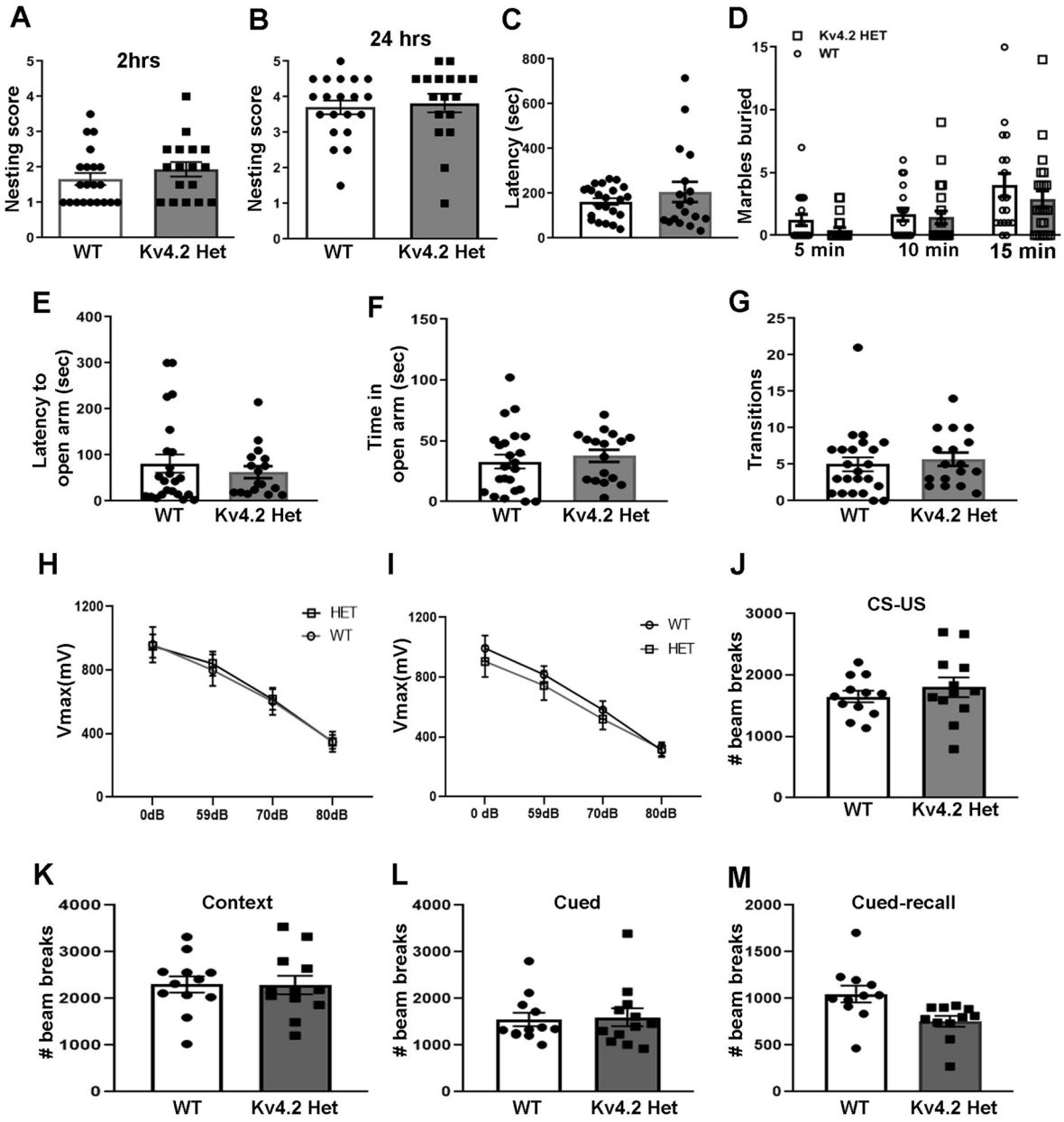

Figure 3: Reduced Kv4.2 does not affect behavior or startle.

(A, B) No change in nesting behavior was observed at 2 h (**A,** WT: n=21; HET: n=17; Mann Whitney test, p=0.278) and 24 h (**B,** WT: n=20; HET: n=17; Mann Whitney test, p=0.436). **(C, D)** In the marble burying assay, no difference in latency to start digging (**C**, WT: n=23; HET: n=18; Mann Whitney test, p=0.77), or in the number of buried marbles at 5, 10 and 15 min of the task were observed (**D**, WT: n=23; HET: n=18; repeated measure 2-way ANOVA, interaction (time × genotype): $F(2,78)=0.80$, $p=0.453$; genotype: $F(1,39)=1.01$, $p=0.322$; time: $F(2,78)=28.20$, $p<0.0001$, no significant differences in pairwise comparisons using Sidak's multiple comparisons test). Data from male mice are shown, results in female mice were similar. **(E-G)** Male Kv4.2^{HET} mice are indistinguishable from WT littermates in latency to enter the open quadrant (**E**, WT: n=23; HET: n=17; Mann Whitney test, p=0.730)

or time spent in the open quadrant (**F**, WT: n=23; HET: n=17; unpaired t-test; t(38)=0.59, p=0.558) or transitions (**G**, WT: n=23; HET: n=17; Mann Whitney test, p=0.357) in the elevated zero maze. **(H, I)** $Kv4.2^{HET}$ mice and WT littermates showed no difference in the Vmax response during the pre-pulse inhibition on day 1 (**H**, WT: n=12; HET: n=12; repeated measure 2-way ANOVA, p (interaction)=0.737, p(genotype)=0.866, p(time)<0.0001) or day 2 (**I,** WT: n=12; HET: n=12; repeated measure 2 way ANOVA, p(interaction)=0.264, p(genotype)=0.631, p(time)<0.0001). **(J-M)** Similarly, no difference was observed in the response to a foot shock paired with tone (unconditioned stimulus, CS-US) (**J**) or in contextual (**K**) or cued trials at 48 (**L**) and 72 hours (**M**) after conditioning. Numbers of photo beam breaks as a measure of movement during the experimental session are shown. Sample sizes were 12 for both genotypes. Error bars represents SEM.

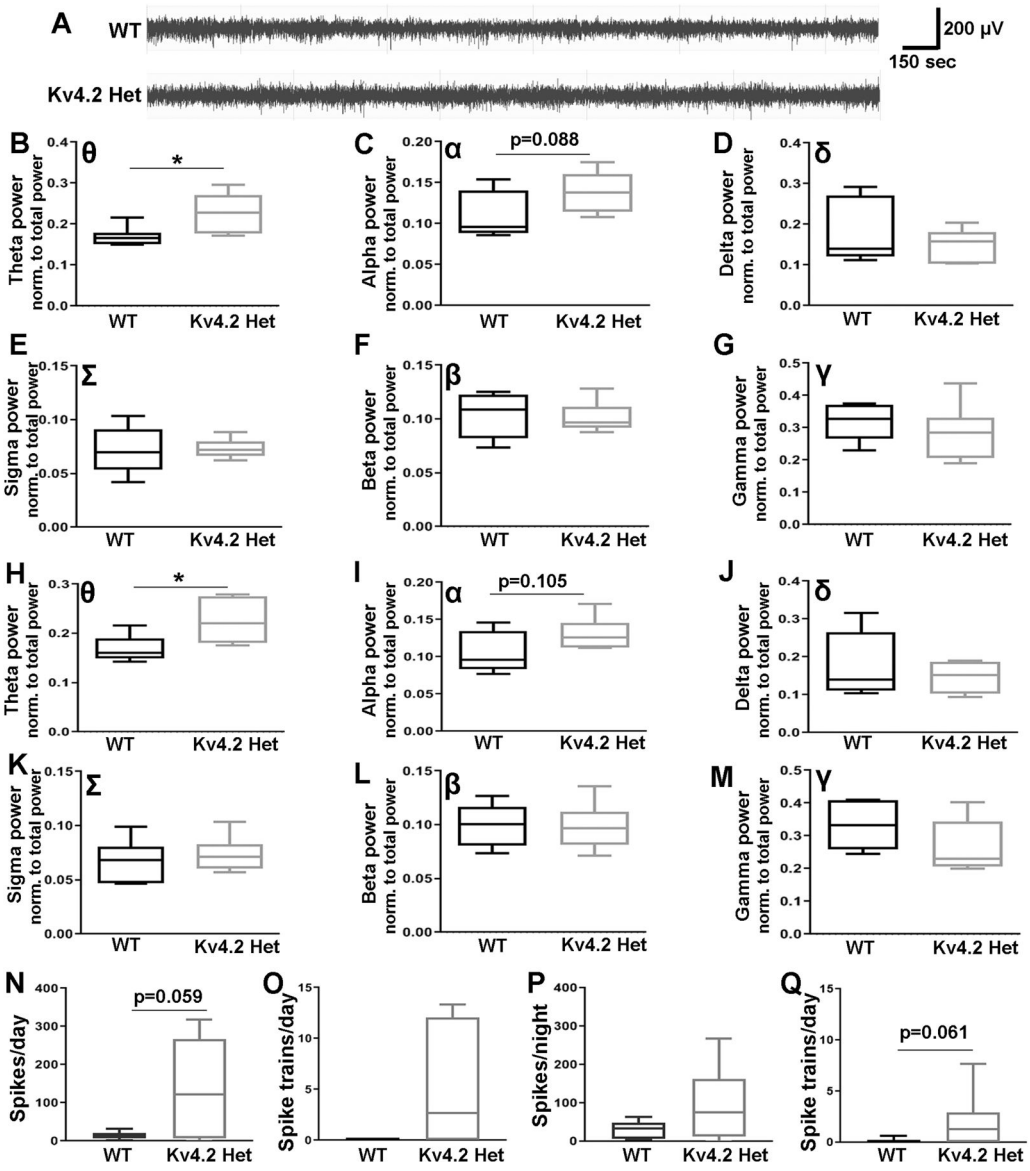

Figure 4: Increased theta power and increased number of electrographic spikes in Kv4.2^{HET} mice.

(A) Representative EEG traces of WT and Kv4.2^{HET} mice. Waveform-specific EEG power analyses during day time showed significantly increased theta waveforms (**B**, Mann Whitney test, *p=0.008), but no significant changes in alpha (**C,** α), delta (**D**, δ), sigma (**E**, Σ), beta (**F**, β) and gamma (**G**, γ) was observed in Kv4.2^{HET} mice compared with WT (unpaired t-tests, **C**: t(10)=1.888, p=0.088; **D**: t(10)=0.178, p=0.443; **E**: t(10)=0.153, p=0.881; **F**: t(10)=0.224, p=0.826; **G**: t(10)=0.775, p=0.456). Likewise, during night time, significantly increased θ waveforms (**H**, unpaired t-test, t(10)=2.701, p=0.022) was observed, but there were no significant changes in α (**I**), δ (**J**), Σ (**K**), β (**L**), and γ (**M**) power (unpaired t-tests, **I**: t(10)=1.780, p=0.105 ; **J:**t(10)=0.773, p=0.457; **K**: t(10)=0.587, p=0.570; **L**: t(10)=0.105, p=0.917; **M**: t(10)=1.482, p=0.169)). Waveform-specific EEG signal was normalized to total power across all waveforms. Shown is the average EGG power during 5-min epochs

from recordings on three consecutive days or nights, respectively. **(N-Q)** Analyses of epileptiform spikes during the day and night time period showed a trend towards increased frequency of spikes during the day but not the night (**N**, day: unpaired t-test, t(10)=2.134, p=0.059 and **P**, night: t(10)=1.514, p=0.161) and of spike trains during the night but not the day (**O**, day: Mann Whitney test, p=0.182; **Q**, night: Mann Whitney test, p=0.061)) in Kv4.2^{HET} mice compared with WT. Sample size was 6 for both genotypes. Examples of spikes and spike trains are shown in Fig. S3. Error bars represent minimum to maximum.

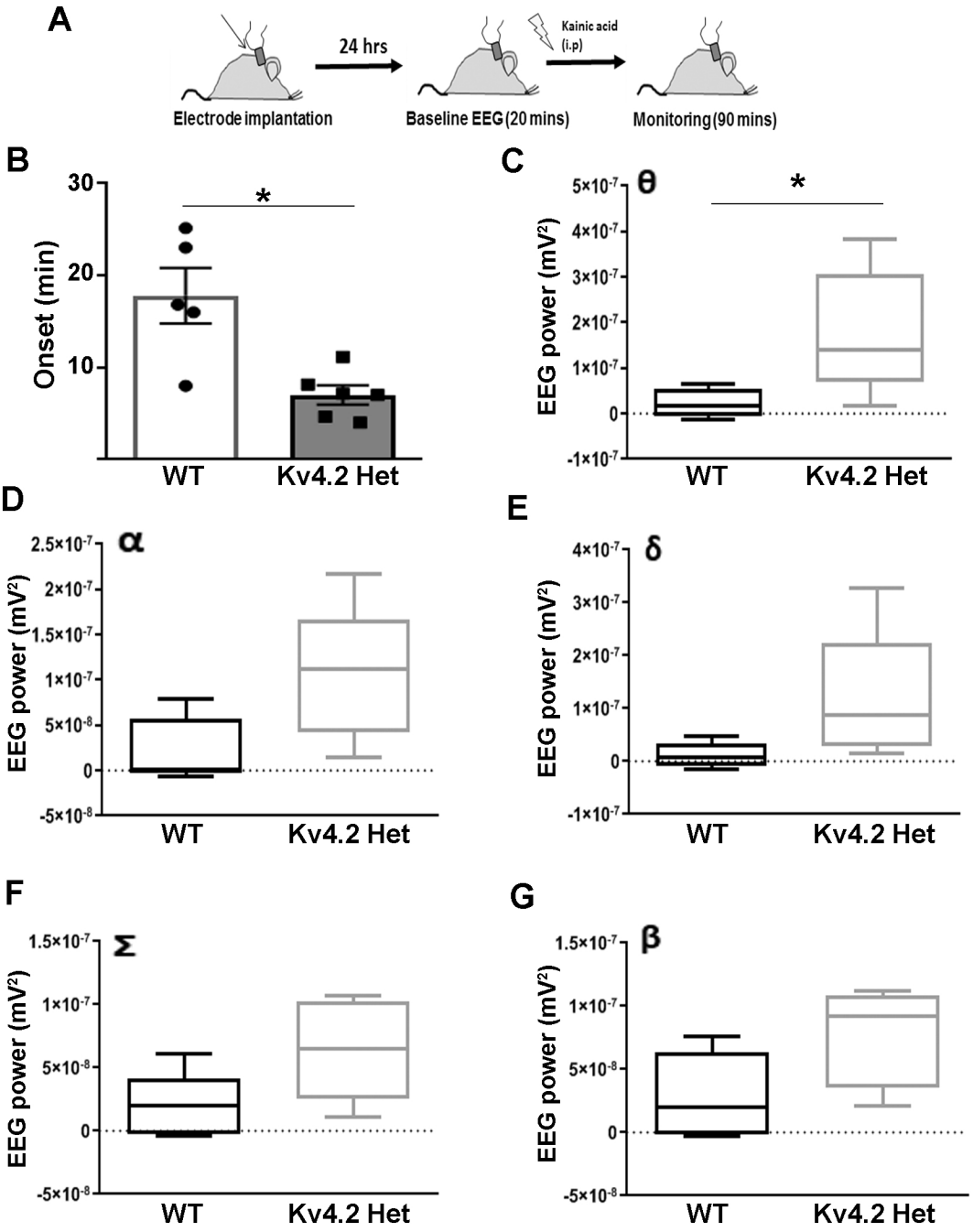

Figure 5: Reduced Kv4.2 levels increase susceptibility to kainic acid-induced seizure.

(A) Timeline depicting time points for electrode implantation and kainic acid injection and EEG recordings. **(B)** Seizure onset analysis post kainic acid showed reduced latency to seizure onset in Kv4.2^{HET} mice compared with WT littermates (WT=5, Het=6; unpaired t-test, t(9)=2.91, *p=0.017). **(C)** EEG power analysis showed significantly increased θ power in the Kv4.2^{HET} mice compared with WT controls (n=5, unpaired t-test, t(8)=2.49, *p=0.037). **(D-G)** No significant change was observed in any of the other waveforms analyzed, (n=5; unpaired t –test, **D**: t(8)=2.27, p(α)=0.052; **E**: t(8)=1.89, p(δ)=0.096; **F**:

t(8)=2.08, p(Σ)=0.071; **G**: t(8)=2.04, p(β)=0.076). However, all EEG waveforms showed a trend towards significantly increased power. Waveform-specific EEG baseline power (prior kainic acid injection) was subtracted from post-injection EEG to normalize for signal intensity. One Kv4.2^{HET} mouse was eliminated from EEG power analysis due to noisy EEG signal. Error bars represent SEM in B, and minimum to maximum in C-G.

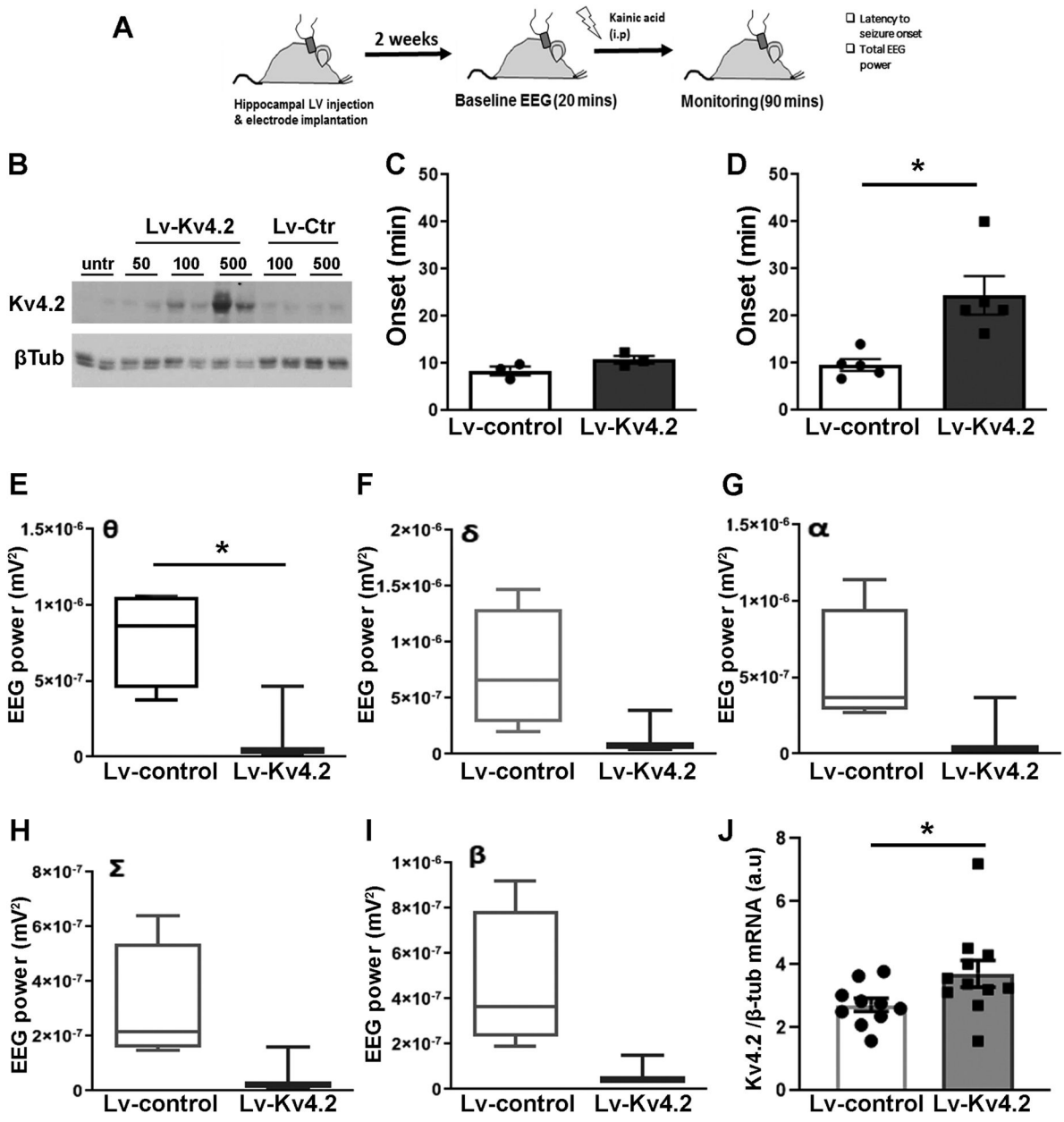

Figure 6: Overexpression of Kv4.2 levels reduces seizure susceptibility.

(A) Timeline depicting the time points for electrode implantation, lentivirus injection and kainic acid injection and EEG recordings. **(B)** Western blot showing lentivirus-mediated overexpression of Kv4.2 in HEK-293 cells. Cells were transfected with increasing amounts of Kv4.2-expressing (*Lv-Kv4.2*) or control (*Lv-Ctr*) virus and assessed for Kv4.2 expression using western blotting three days later. Numbers indicate multiples of 1000 transfective units. **(C)** A lower dose of Kv4.2-expressing lentivirus (1 μl/side = ~100,000 transfective units/side) has no effect on seizure onset (8–9 week-old males injected with 15 mg/kg kainic acid two weeks after virus injection; n = 3; unpaired t-test, t(4) = 1.91, p = 0.129). **(D)** Double dose (2 μl/side = ~200,000 transfective units/side) of hippocampal injections of Kv4.2-expressing lentivirus significantly increases the latency to kainic acid-induced seizure

(n = 5; unpaired t-test, t(8) = 3.47, *p = 0.008). **(E)** θ power was decreased in Kv4.2 overexpressing mice during the first 90 min after kainic acid injection (baseline subtracted; ctr: n = 4; Kv: n = 3; unpaired t-test, t(5) = 2.69, *p = 0.043). (Fsingle bondI) No significant difference was observed in other EEG waveforms (unpaired t-tests, **F**: t(5) = 1.75, p(δ) = 0.140), **G**: t(5) = 1.54, p(α) = 0.183, **H**: t(5) = 1.72, p(Σ) = 0.146; **I**: t(5) = 2.03, p(β) = 0.098). **(J)** Lentivirus-mediated Kv4.2 mRNA overexpression in the hippocampus was confirmed by qRT-PCR on hippocampal tissue punches (ctr: n = 11; Kv4.2: n = 10; Mann-Whitney test, *p = 0.038). Error bars represent SEM in C, D and J, and minimum to maximum in E-I.